Using Water-Quality Profiles to Characterize Seasonal Water Quality and Loading in the Upper Animas River Basin, Southwestern Colorado

By Kenneth J. Leib, M. Alisa Mast, and Winfield G. Wright

U.S. GEOLOGICAL SURVEY

Water-Resources Investigations Report 02–4230

Prepared in cooperation with the
BUREAU OF LAND MANAGEMENT

Denver, Colorado
2003

U.S. DEPARTMENT OF THE INTERIOR
GALE A. NORTON, Secretary

U.S. GEOLOGICAL SURVEY
Charles G. Groat, Director

For additional information write to:

District Chief
U.S. Geological Survey
Box 25046, Mail Stop 415
Denver Federal Center
Denver, CO 80225–0046

Copies of this report can be purchased from:

U.S. Geological Survey
Information Services
Box 25286
Denver Federal Center
Denver, CO 80225

CONTENTS

FIGURES

TABLES

CONVERSION FACTORS, DEFINITIONS, AND ABBREVIATIONS

Multiply	By	To obtain
foot (ft)	0.3048	meter (m)
mile (mi)	1.609	kilometer (km)
square mile (mi^2)	2.590	square kilometer (km^2)
gallon (gal)	3.785	liter (L)
cubic foot per second (ft^3/s)	0.02832	cubic meter per second (m^3/s)
cubic foot per second per square mile [$(ft^3/s)/mi^2$] or cfsm	0.01093	cubic meter per second per square kilometer [$(m^3/s)/km^2$]
pound per day (lb/d)	0.4536	kilogram per day (kg/d)

Temperature in degrees Celsius (°C) may be converted to degrees Fahrenheit (°F) as follows:

$$°F = 1.8\ (°C) + 32$$

Water Year: A 12-month period beginning October 1 and ending September 30 of the following year. Water year is defined by the calendar year in which it ends.

Additional Abbreviations

α	the regression coefficient that is the intercept in the regression model
β	constant beta used in hyperbolic transformation
B and B_n	coefficient of explanatory variables in multiple regression
C_Q	constituent concentration in milligrams per liter
DV_1	dummy variable
J_C	first-order julian date transformation
J_D	second-order julian date transformation
J_E	third-order julian date transformation
J_F	fourth-order julian date transformation
X_Q	streamflow in cubic feet per second
X_h	transformed streamflow
r^2	the coefficient of determination
µg/L	micrograms per liter
µm	micrometer
µS/cm	microsiemens per centimeter at 25 degrees Celsius
mg/L	milligrams per liter

Acronyms

USGS	U.S. Geological Survey
CDMG	Colorado Division of Minerals and Geology
CDPHE	Colorado Department of Public Health and Environment
BOR	Bureau of Reclamation
CRW	Colorado River Watch Program
SGC	Sunnyside Gold Corporation
EDTA	ethylenediaminetetraacetate
ICP-AES	inductively coupled atomic emission spectroscopy
GFAA	graphite furnace atomic absorption spectroscopy
AAS	atomic absorption spectroscopy
MRL	minimum reporting level

Using Water-Quality Profiles to Characterize Seasonal Water Quality and Loading in the Upper Animas River Basin, Southwestern Colorado

By Kenneth J. Leib, M. Alisa Mast, *and* Winfield G. Wright

Abstract

One of the important types of information needed to characterize water quality in streams affected by historical mining is the seasonal pattern of toxic trace-metal concentrations and loads. Seasonal patterns in water quality are estimated in this report using a technique called water-quality profiling. Water-quality profiling allows land managers and scientists to assess priority areas to be targeted for characterization and(or) remediation by quantifying the timing and magnitude of contaminant occurrence.

Streamflow and water-quality data collected at 15 sites in the upper Animas River Basin during water years 1991–99 were used to develop water-quality profiles. Data collected at each sampling site were used to develop ordinary least-squares regression models for streamflow and constituent concentrations. Streamflow was estimated by correlating instantaneous streamflow measured at ungaged sites with continuous streamflow records from streamflow-gaging stations in the subbasin. Water-quality regression models were developed to estimate hardness and dissolved cadmium, copper, and zinc concentrations based on streamflow and seasonal terms. Results from the regression models were used to calculate water-quality profiles for streamflow, constituent concentrations, and loads.

Quantification of cadmium, copper, and zinc loads in a stream segment in Mineral Creek (sites M27 to M34) was presented as an example application of water-quality profiling. The application used a method of mass accounting to quantify the portion of metal loading in the segment derived from uncharacterized sources during different seasonal periods. During May, uncharacterized sources contributed nearly 95 percent of the cadmium load, 0 percent of the copper load (or uncharacterized sources also are attenuated), and about 85 percent of the zinc load at M34. During September, uncharacterized sources contributed about 86 percent of the cadmium load, 0 percent of the copper load (or uncharacterized sources also are attenuated), and about 52 percent of the zinc load at M34. Characterized sources accounted for more of the loading gains estimated in the example reach during September, possibly indicating the presence of diffuse inputs during snowmelt runoff. The results indicate that metal sources in the upper Animas River Basin may change substantially with season, regardless of the source.

INTRODUCTION

The upper Animas River Basin (the Animas Basin) (fig. 1) is a mineralized region of the San Juan Mountains in southwestern Colorado where gold, silver, and other base metals were mined from the late 1800's to 1992. As a result of historical mining activities, many streams in the Animas Basin have high concentrations of dissolved metals, which have caused a reduction or elimination of fish and invertebrate communities (Besser and Leib, 1999).

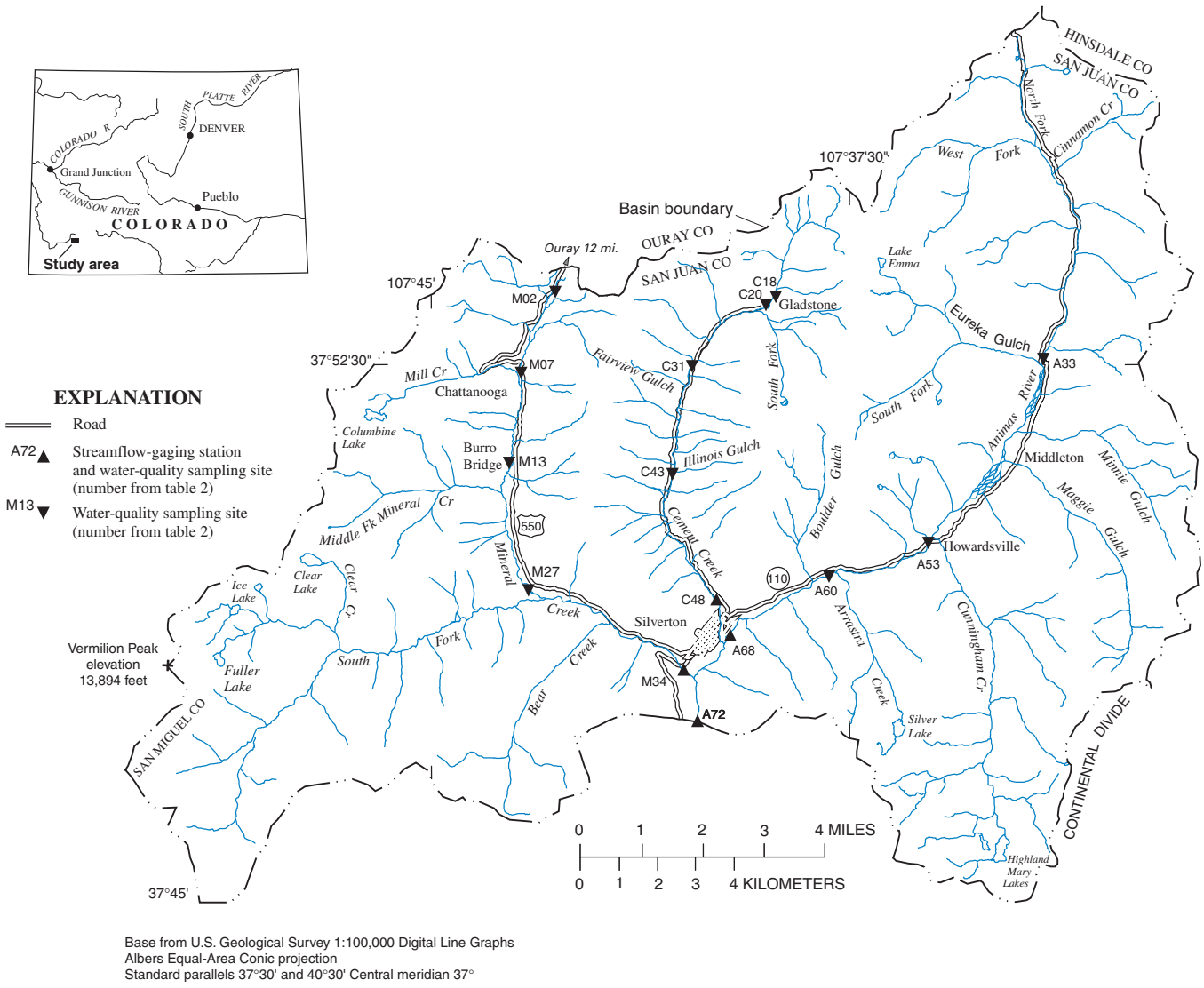

Figure 1. Streamflow-gaging stations and water-quality sampling sites in the upper Animas River Basin.

Since 1991, various government agencies have established initiatives which, through collaborative efforts, seek to assess the effects of historical mining on water quality in the basin. Included in these efforts is the U.S. Department of the Interior Abandoned Mine Lands Initiative. As part of this initiative, the U.S. Geological Survey (USGS) has provided technical assistance in support of actions by Federal land-management agencies to improve water quality in contaminated stream systems associated with inactive hard-rock mining activities. These efforts are important because cost-efficient remediation requires a thorough understanding of the extent and cause of water-quality degradation and because instream water-quality standards are being proposed by the Colorado Department of Public Health and Environment to comply with the 1977 Clean Water Act.

One of the important types of information needed to characterize water quality in streams affected by historical mining are seasonal and spatial patterns of toxic metal concentrations and loads. Typically, the concentrations of most dissolved constituents in streams decrease during periods of high streamflow and increase during base flow (Anderson and others, 1997). An understanding of when trace-metal concentrations are highest improves the ability

of biologists to evaluate the potential changes to the health of aquatic ecosystems. Biologists are interested in periods of highest trace-metal concentrations because this is when aquatic species are most vulnerable, particularly those in sensitive life-cycle development stages. Land managers may be more interested in knowing what areas contribute the largest trace-metal loads in order to assess where remediation would be most effective. Because the largest trace-metal loads generally occur during periods of highest streamflow and the highest concentrations occur during periods of low streamflow, it is important to characterize seasonal concentration patterns over an entire annual cycle.

Several years of sample collection often are needed to adequately characterize an annual water-quality cycle because wet, dry, and normal years may have dissimilar water-quality patterns. A long-term water-quality database exists for the Animas Basin and was used as a starting point for quantifying seasonal water-quality patterns at gaged and ungaged sites in the drainage basin. This database, although extensive, could not provide accurate estimates of annual water-quality cycles due to the gaps between sampling periods. Some continuous estimate of water quality, including streamflow and concentration derived from the existing data, was needed. Therefore, selected data sets were expanded using statistical inference to provide estimated data during periods when no data were collected. In doing this, a more complete estimate of the annual range and timing of constituent concentrations and loads could be reported because more information was made available. This report summarizes how statistical modeling is used to define water quality in main-stem streams of the Animas Basin as part of a technique for presenting watershed-scale information in areas affected by historical mining.

Purpose and Scope

The purpose of this report is to characterize spatial and seasonal variability of water quality in the Animas Basin using a technique called water-quality profiling. Water-quality profiling is similar to traditional seasonal water-quality characterization techniques in which solute concentrations and loads are estimated with regression modeling (Searcy, 1959; Steele, 2000). In addition, water-quality profiling combines data from multiple sites to provide information about concentrations and loads along the elevational gradient of a stream. Hence, water-quality profiles depict seasonal differences in water quality at multiple sampling locations in one concise and informative graph. Water-quality profiles quantify the timing and extent of contaminant occurrence and can aid land managers and scientists in determining priority areas to be targeted for characterization and possible remediation. Thus, the water-quality profile presents a useful way to package information from large and complicated data sets in a format that is easily interpreted. A description of how this technique has been applied to water-quality data from the Animas Basin study is included.

The objectives of this report are to (1) describe the methods used to derive water-quality profiles; (2) compute water-quality profiles for 15 sampling sites in the Animas Basin for streamflow, hardness, and dissolved cadmium, copper, and zinc concentrations that represent current water-quality conditions in the basin; (3) discuss results of water-quality profiling; and (4) present an example application of results from water-quality profiling.

Methodology and interpretation contained in this report are intended to guide future water-quality studies that seek to quantify effects from multiple contamination sources under varying hydrologic conditions. In addition, an understanding of the seasonal patterns of hardness should improve estimates of metals toxicity because hardness is used in numerous equations to determine regulatory standards (see Appendix). Hardness is included in many standard calculations because it possesses properties that decrease the toxic effects of certain constituents including cadmium, copper, and zinc.

Description of Study Area

The upper Animas River Basin encompasses about 146 mi^2 of rugged terrain in the San Juan Mountains of southwestern Colorado (U.S. Geological Survey, 2000). Elevations in the basin range from 9,200 ft near the town of Silverton, Colo., to nearly 13,900 ft at the summit of Vermilion Peak (fig. 1). The upper part of the river has a channel length of about 15.5 mi upstream from streamflow-gaging station 09359020 (site A72) and an average gradient of about 184 ft/mi. Major tributaries to the upper Animas River are Mineral and Cement Creeks, which represent

about 50 percent of the Animas Basin drainage area. Climate in the area is characterized by long, cold winters and short (3 to 4 months), cool summers. Average monthly air temperature at Silverton ranges from 16°F in January to 55.3°F in July. Precipitation averages 45 inches annually, of which about 70 percent accumulates in a seasonal snowpack between November and April (Colorado Climate Center, 2000). Most of the remaining precipitation falls during monsoonal thundershowers in late summer and early fall. The Animas Basin lies in the Southern Rocky Mountain ecoregion (Bailey and others, 1994), with much of the area lying above treeline. Areas below treeline typically are vegetated by dense stands of subalpine Engelmann spruce and subalpine fir.

Hydrology

Flow in the upper Animas River originates primarily from melting snowpack. Snowpack ranges from 10 to 20 ft in depth and averages 10 to 50 percent water content depending on season (Colorado Climate Center, 2000). Variations in annual snowpack are reflected in the magnitude and duration of snowmelt runoff each year. Figure 2 shows how the annual peak and duration of snowmelt runoff at sampling site A72 varied during the study period (water years 1992 to 1999). Streamflow patterns at site A72 are representative of streamflow patterns at the other gaging stations in the study area. Peak flows in the Animas Basin generally occur from late May to early July. Maximum daily mean streamflow for the study period occurred

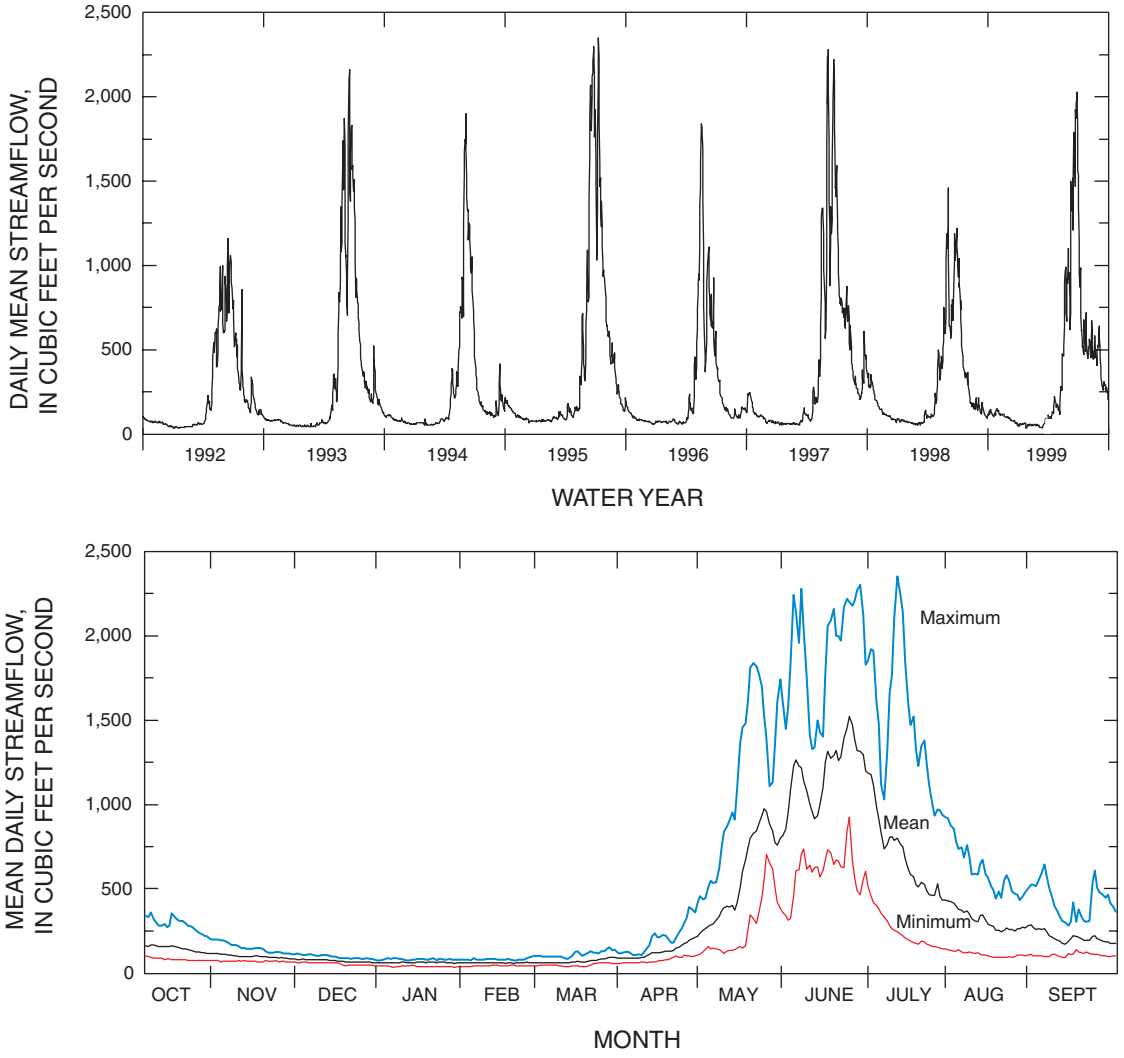

Figure 2. Daily mean streamflow and maximum, minimum, mean daily streamflow at site A72, water years 1992 to 1999.

on June 10, 1995, at 2,350 ft^3/s. Minimum daily mean streamflow for the study period occurred on January 2, 1992, at 35 ft^3/s. This low streamflow condition was caused by freezing temperatures in winter, when the main source of streamflow is ground water. Streamflow derived from monsoonal thunderstorms in late summer and fall typically do not exceed peak snowmelt volumes in the spring. However, the USGS (2000) suggests that historical peak flooding at site A72 occurred October 5, 1911, as a result of sustained high-intensity thunderstorms in the region.

A pattern measured in many streams is a tendency for water during a rising stage to have a considerably higher concentration than water passing a sampling point at an equal flow rate after peak discharge has passed (Hem, 1985). This condition is referred to as "hysteresis" and has been documented in the Animas Basin by Wirt and others (1999) for localized storm runoff events in Cement Creek. Besser and Leib (1999) also observed annual hysteresis in the upper Animas River and found that concentrations of dissolved zinc and copper, during the rising limb of the snowmelt hydrograph, can be two or three times those that occur at similar flow rates during the receding portion of the snowmelt hydrograph. In addition, concentrations of zinc and copper tended to increase during periods of base flow (November–March) with little variation in streamflow. Figure 3 illustrates the hysteretic pattern at A72 for dissolved zinc in water year 1997. This plot illustrates the clockwise progression that dissolved zinc concentration takes throughout the water year, where dissolved zinc is operationally defined as the concentration remaining in 0.45-µm filtrate. During base flow, concentrations increase despite little or no decrease in streamflow. During the rising limb of the snowmelt hydrograph (April–June), concentrations are diluted; however, concentrations during the rising limb are not as dilute as concentrations on the falling limb of the snowmelt hydrograph (July–October). The pattern for zinc is typical for other trace metals as well as for other sampling sites in the Animas Basin. Because a hysteretic cycle is typical of concentration patterns in the Animas Basin, it is possible to correlate not only streamflow discharge to constituent concentration but also time (periodicity). These correlations form the foundation from which water quality will be estimated in this report.

Geology

The rocks of the upper Animas River Basin are mineralized as a result of the emplacement of the ancient Silverton Caldera, which was the second of two volcanoes that collapsed and formed cylindrical pits (or calderas) about 26 million years ago (Varnes, 1963; Luedke and Burbank, 1996). Lava was deposited within and around the caldera, and volcanic ashes accumulated in thick deposits throughout the region. Doming and collapse of the Silverton Caldera were accompanied by the development of numerous faults and fracture zones, which acted as a plumbing system for later circulation of hot, acidic fluids that contained large amounts of dissolved copper, gold, lead, manganese, silica, sulfur, and zinc (Casadevall and Ohmoto, 1977). As these ore fluids cooled near the land surface, minerals were precipitated in the faults, forming veins. The ore fluids also altered and leached the surrounding host rocks. Some of the rocks in the basin were highly altered and mineralized by a combination of intrusive magma bodies (molten rock that never breached the land surface) and the circulation of hot, mineral-rich fluids.

Within the caldera boundary, veins of disseminated pyrite are present throughout the volcanic rocks. Water draining from the mineralized bedrock can be acidic and can have high concentrations of dissolved minerals (Mast and others, 2000). Outside the caldera boundary, veins are less common and the rocks usually contain greater amounts of calcium carbonate, which tends to buffer the water in streams and mine drainage.

Mines and prospects also can affect the water quality of streams: mining leads to an increase in weathering rates because minerals in the mines are exposed to oxygen on freshly broken rock surfaces as air moves through the mines. The exposure to the oxygen changes the chemical makeup of some of the minerals into forms that more readily dissolve in water; therefore, high concentrations of dissolved minerals are present in water that drains from some mines. Mines also can divert ground water from its premining flow path, and the water can be collected into a single discharge at the mine entrance. Hence, the water flow and quality in the vicinity of a mine can be affected.

Mine-Site Remediation

Mining in the San Juan Mountains has left a legacy of abandoned mine sites as sources of acidic mine drainage. The majority of sites in the Animas Basin have been inventoried and some priority mines

are slated for remediatory action. This remediation work has the potential to alter water quality at downstream sampling sites, thus complicating any interpretation of the data. For this reason, it was necessary to document the completion date and location of remediation projects in the Animas Basin. Later in the report, this information will be used for trend analysis to determine which data sets or portions of data sets represent stable water-quality conditions.

Based on the limited number of remediation projects completed at the time this report was written (2000), trends (if any) in water quality were assumed to be related to mined-land remediation done by Sunnyside Gold Corporation (SGC). SGC, through an agreement signed in May 1996 with the Colorado Department of Public Health and Environment, Water-Quality Control Division, closed the valves on bulkhead seals placed in mines located in Cement Creek and tributaries to the

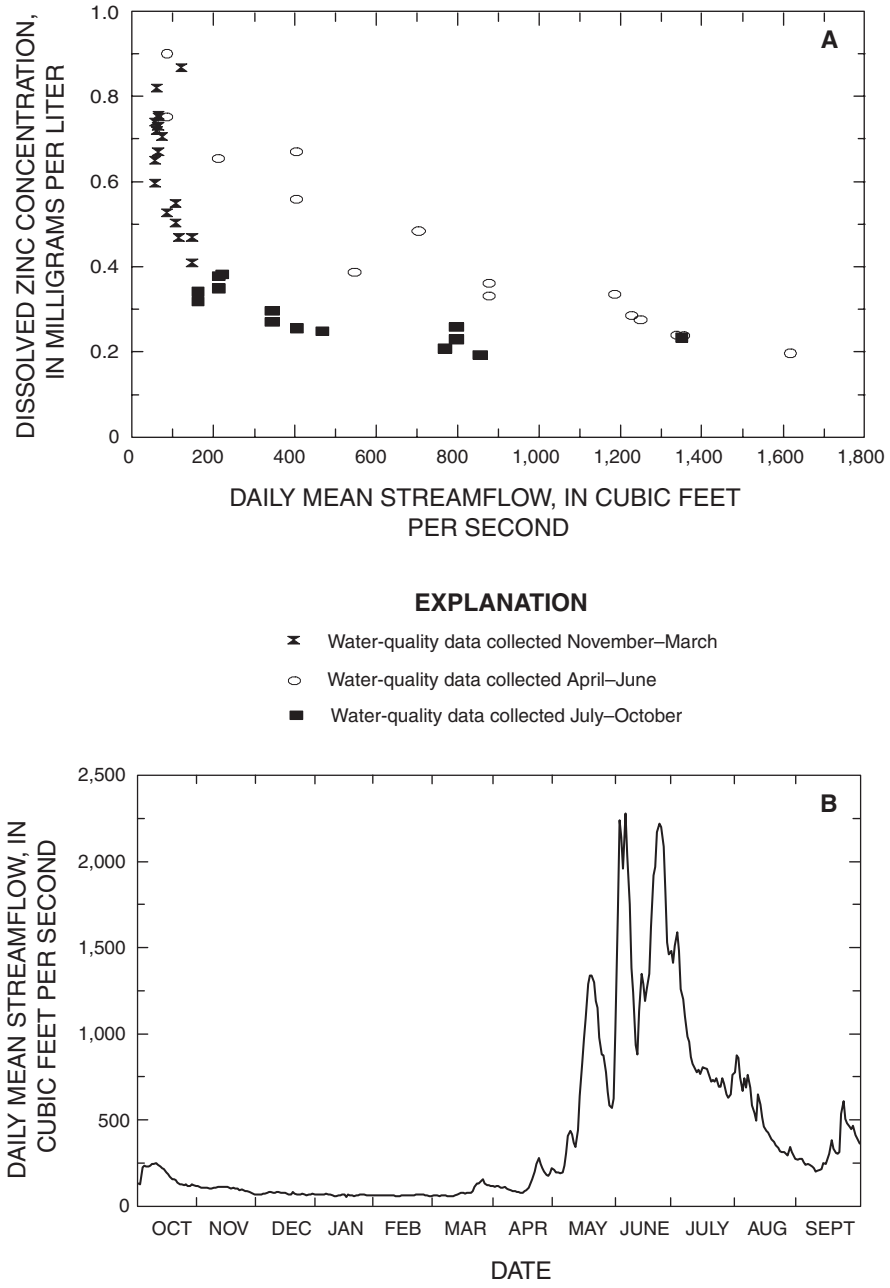

Figure 3. (A) Dissolved zinc concentration related to daily mean streamflow; and (B) daily mean streamflow, sampling site A72, water year 1997.

Animas River and also removed and(or) covered selected mine wastes (Colorado Department of Public Health and Environment, 1995). Beginning in 1996, SGC also treated the majority of streamflow in Cement Creek during periods of base flow between sites C18 and C20 by using settling ponds to precipitate metals in solution. Most of these projects and many other smaller ones were completed in the summer of 1997; however, other maintenance work and mined-land remediation is ongoing in the Animas Basin by SGC and an increasing number of Federal and private parties. Completion dates for Federal and private party projects (excluding SGC) were not compiled and considered in this study because of the small number and small size of each project relative to the SGC projects. Table 1 lists dates and locations for mined-land remediation projects that were performed by SGC (Larry Perino, Sunnyside Gold Corporation, written commun., 2000) and were used in this study to correlate to possible trends in water quality.

Acknowledgments

The authors thank Sunnyside Gold Corporation, the Animas River Stakeholders Group, and the Bureau of Reclamation for data contributed for this analysis. The authors also thank David Nimick and Richard Hooper for technical reviews; Mary Kidd for editorial review; Michael Karlinger, Briant Kimball, and Kernell Ries for technical assistance; Jonathan Evans, Jedd Sondergard, David Grey, and Mark Gress for field assistance; and James Bennett, David Grey, and Mark Gress for maintaining the streamflow-gaging stations.

METHODS OF DATA COLLECTION

Water-quality data presented in this report were collected by seven groups and government agencies. During water years 1991 to 1999, water-quality data were collected by the Colorado Department of Health and Environment (CDPHE), Sunny Side Gold Corporation (SGC), Colorado Division of Minerals and Geology (CDMG), Colorado River Watch (CRW), and the Bureau of Reclamation (BOR). Water-quality data also were collected by the USGS during water years 1997 to 1999, in cooperation with the Bureau of Land Management (BLM), as part of a national interdepartmental initiative to provide essential information for mine cleanups planned by land-management agencies in the Western United States (Nimick and von Guerard, 1998). Beginning in November 1996, all data-collection efforts by the USGS were conducted in collaboration with the Animas River Stakeholders Group (ARSG), which consists of citizens, landowners, members of the mining industry, and representatives from State and Federal agencies. The ARSG compiles and stores all available water-quality data in the Animas Basin for purposes of scientific interpretation and land-management decision making. The ARSG database for the Animas Basin, which was the main source of data for this study, resides on the World Wide Web (Animas River Stakeholders Group, 2000). Data collected by the USGS are reported in Mast and others (2000). Continuous streamflow data used in this report were obtained by the USGS. This streamflow information is also available on the Internet (U.S. Geological Survey, 1991–2000, URL: http://waterdata.usgs.gov/co/nwis/).

Table 1. Summary of major mined-land remediation projects in the upper Animas River Basin

Project	Completion date	Downstream sampling sites	Subbasin
American Tunnel bulkhead closure	September 9, 1996	C20, C31, C43, C48, A72	Cement Creek
Cement Creek treatment	Ongoing	C20, C31, C43, C48, A72	Cement Creek
Terry Tunnel bulkhead closure	July 17, 1996	A53, A60, A68, A72	Upper Animas River
Lead Carbonate and American Tunnel mine waste dump removal	Fall 1995	C31, C43, C48, A72	Cement Creek
Eureka mill tailings removal	Fall 1996	A53, A60, A68, A72	Upper Animas River
Ransom Tunnel bulkhead	June 1997	A53, A60, A68, A72	Upper Animas River
Boulder Creek tailings removal	June 1997	A68, A72	Upper Animas River
Gold Prince project	September 1997	A33, A53, A60, A68, A72	Upper Animas River
Longfellow/Koehler project	Fall 1997	M02, M07, M13, M27, M34, A72	Mineral Creek
Pride of the West tailings removal	Fall 1997	A53, A60, A68, A72	Upper Animas River
Mayflower mill diversion project	Fall 1999	A68, A72	Upper Animas River
Tailings pond surface and ground-water drainage project	December 1999	A68, A72	Upper Animas River

Water-Quality Sampling Sites

Fifteen sampling sites on the Animas River or its two major tributaries (Cement and Mineral Creeks) were selected in 1997 for inclusion in this study (table 2). Four of these sites were gaging stations with continuous streamflow record. The sites were in the downstream portion of the Animas Basin; two were at the mouths of Cement and Mineral Creeks and two were on the Animas River—one upstream from Cement Creek and the other downstream from Mineral Creek. These gaged sites were selected because the continuous streamflow record was needed to estimate streamflow at ungaged sites. These sites also had an extensive record of water-quality data (32 to 112 samples). Eleven ungaged sites in the middle and upper parts of the Animas Basin also were selected because their locations bracketed major mining-related sources of metals and because some water-quality data were already available. Additional water-quality data (Mast and others, 2000; Animas River Stakeholders Group, 2000) were collected at some sites during water years 1997–99 to ensure that sufficient data for statistical modeling were available for all sites.

Table 2. Descriptive information for sampling sites

[mi^2, square miles]

Sampling site name	Sampling site number (fig. 1)	Latitude and longitude	Drainage area (mi^2)	Percentage of upper Animas River drainage basin	River mile (distance downstream from respective subbasin headwaters)	Streamflow-gaging station number
Cement Creek upstream from Gladstone	C18	37°53'26" 107°38'55"	3.0	2.1	2.7	Ungaged
Cement Creek near Gladstone	C20	37°53'23" 107°39'08"	3.1	2.1	2.9	Ungaged
Cement Creek downstream from Fairview Gulch	C31	37°52'31" 107°40'17"	9.44	6.5	4.5	Ungaged
Cement Creek downstream from Illinois Gulch	C43	37°50'50" 107°40'38"	14.8	10.1	6.3	Ungaged
Cement Creek at Silverton	C48	37°49'11" 107°39'47"	20.1	13.8	9.2	09358550
Mineral Creek near headwaters	M02	37°53'40" 107°42'48"	0.10	0.1	0.15	Ungaged
Mineral Creek at Chattanooga	M07	37°52'27" 107°43'26"	4.4	3.0	1.8	Ungaged
Mineral Creek at Burro Bridge	M13	37°51'02" 107°43'31"	10.4	7.1	3.5	Ungaged
Mineral Creek upstream from South Fork Mineral Creek	M27	37°49'16" 107°13'08"	20.0	13.7	5.9	Ungaged
Mineral Creek at Silverton	M34	37°48'10" 107°40'20"	52.4	35.9	9.0	09359010
Animas River at Eureka	A33	37°52'45" 107°33'55"	18.2	12.5	6.2	Ungaged
Animas River at Howardsville	A53	37°50'07" 107°35'52"	57.7	39.5	10.1	Ungaged
Animas River near Arrastra Gulch	A60	37°49'38" 107°37'34"	60.0	41.1	12.1	Ungaged
Animas River at Silverton	A68	37°48'40" 107°39'31"	70.6	48.4	14.3	09358000
Animas River downstream from Silverton	A72	37°47'25" 107°40'01"	146	100	16.0	09359020

Sample Collection and Laboratory Analysis

Sample collection protocols and laboratory analytical methods differed slightly among agencies and groups; however, there was a concerted effort, coordinated by the ARSG, to adopt common sample collection protocols, compare laboratory analytical methods, and collect concurrent replicate samples for comparison of results among laboratories. Brief descriptions of the different methods for collection of water-quality samples are listed in table 3. Most stream samples were collected with depth-integrated samplers using the equal-width-increment method (EWI), except during high-flow conditions when grab sampling was occasionally used for safety reasons (Edwards and Glysson, 1988). Each water-quality sample was collected at approximately the same time the streamflow measurements were taken.

Water-quality samples were filtered with 0.45-µm filters by all groups. Polyethylene bottles were used by all participants for sample collection and shipment to the laboratory. Concentrated nitric acid was used by all participants for preservation of water-quality samples for cation and trace-metal analyses. Powderless surgical gloves were worn by all participants during collection of water-quality samples. A detailed description of USGS water-sample collection methods is presented in Mast and others (2000).

Laboratory methods used for analysis of water-quality samples and the analytical detection limits differed among agencies and groups. The different analytical methods and detection limits for each element are listed in table 4. Quality-assurance procedures used by all participants included rigorous cleaning of sampling equipment and sample bottles and collection of quality-control samples (field-equipment blanks and replicate samples). Comparison of selected quality-control samples collected by the USGS is presented in Mast and others (2000). The results indicate that the analytical precision for the majority of replicate samples collected by the USGS was ±8 percent. In addition, field-equipment blanks did not show any constituent contamination from the methods used in this study. Agencies and groups who contributed data to the ARSG for use in this analysis were quality assured by the participating agency as well as the ARSG watershed coordinator. No major problems with water-quality collection and precision were reported. Concurrent replicates were collected on two occasions by the USGS and ARSG groups as a check for any possible differences in constituent concentrations resulting from the differences in collection method and(or) laboratory procedures (Wilde and Radtke, 1997). Results of concurrent replicate sampling indicated that constituent concentrations reported by any given party were within ±10 percent. Quality-assurance information for the various other agencies and groups that collected data in coordination with the ARSG, and for use in this study, is available on the Internet (Animas River Stakeholders Group, 2000).

Table 3. Methods of sample collection for water-quality data collected in the upper Animas River Basin

[USGS, U.S. Geological Survey; BOR, Bureau of Reclamation; CDMG, Colorado Division of Minerals and Geology; CDPHE, Colorado Department of Public Health and Environment; CRW, Colorado River Watch Program; SGC, Sunnyside Gold Corporation; EWI, equal-width-increment method; µm, micrometer]

Participant	Method of water-sample collection	Streamflow determination	Filtration method
USGS	EWI wading during low flow EWI from cableway or bridge during high flow	Wading the stream during low flow; from cableway or bridge during high flow	0.45-µm plate filter, cartridge filter
BOR	EWI wading during low flow EWI from cableway or bridge during high flow	Streamflows obtained from streamflow-gaging stations	0.45-µm plate filter
CDMG	EWI wading during low flow Grab sample from bridge during high flow	Wading the stream during low flow; from cableway or bridge during high flow	0.45-µm syringe filter
CDPHE	EWI wading during low flow Grab sample from bridge during high flow	Wading the stream during low flow	0.45-µm syringe filter
CRW	Grab sample from bridge during low and high flow; bucket in centroid of flow	Streamflows obtained from streamflow-gaging stations	0.45-µm syringe filter
SGC	EWI wading during low flow Grab sample from bridge during high flow	Streamflows obtained from streamflow-gaging stations, flumes, and wading during low flow	0.45-µm plate filter

Table 4. Analytical methods and minimum reporting limits for water-quality data collected in the upper Animas River Basin

[USGS, U.S. Geological Survey; CDMG, Colorado Division of Minerals and Geology; CDPHE, Colorado Department of Public Health and Environment; BOR, Bureau of Reclamation; CRW, Colorado River Watch Program; SGC, Sunnyside Gold Corporation; EDTA, ethylenediaminetetraacetate; ICP-AES, inductively coupled atomic emission spectroscopy; GFAA, graphite furnace atomic absorption spectroscopy; AAS, atomic absorption spectroscopy; Ca+Mg, summation method in terms of calcium carbonate; titration, gravimetric titration; µg/L, micrograms per liter; mg/L, milligrams per liter; $CaCO_3$, calcium carbonate]

Analyte	Method						Minimum reporting level						Units
	USGS	CDMG	CDPHE	BOR	CRW	SGC	USGS	CDMG	CDPHE	BOR	CRW	SGC	
Cadmium	ICP-AES, GFAA	ICP-AES	ICP-AES	GFAA	ICP-AES	GFAA	2, 0, 0.02	3	3	0.3	3	1	µg/L
Calcium	ICP-AES, AAS	ICP-AES	ICP-AES	GFAA	ICP-AES	ICP-AES, AAS	0.15, 0.1	0.2	1	0.2	0.2	1	mg/L
Copper	ICP-AES, GFAA	ICP-AES	ICP-AES	GFAA	AAS	GFAA	4	1	4	5	1	3	µg/L
Magnesium	ICP-AES, AAS	ICP-AES	ICP-AES	GFAA, AAS	Titration	ICP-AES, AAS	0.01	1	1	0.2	1	1	mg/L
Hardness	(Ca+Mg)	(Ca+Mg)	Titration (EDTA)	(Ca+Mg)	(Ca+Mg)	Titration (EDTA)	1	1	1	0.2	1	1	mg/L (as $CaCO_3$)
Zinc	ICP-AES	ICP-AES	ICP-AES	GFAA	AAS	ICP-AES, AAS	20	20	8	10	10	10	µg/L

Hardness values reported by each group are defined as the total concentration of calcium and magnesium ions in units of milligrams per liter as calcium carbonate. Analytical methods used to determine hardness values are listed in table 4.

Streamflow Regression Models

Streamflow regression models were developed to provide estimated values of daily mean streamflow at ungaged sampling sites. The streamflow models were developed by regressing daily mean streamflow at gaged sampling sites with instantaneous streamflow measured at ungaged sites. Sites C18, C20, C31, and C43 in Cement Creek were correlated to site C48; sites M02, M07, M13, and M27 in Mineral Creek were correlated to site M34; and sites A33, A53, A60, and A68 in the Animas River were correlated to site A72. Sites A33, A53, and A60 were correlated to site A72 rather than site A68 (a gaged site on the Animas) because the correlation was better at A72.

During water years 1991–99, 10 to 20 streamflow measurements at each ungaged site were obtained during different streamflow conditions. Up to four measurements at each of the ungaged sites were obtained from 1991 to 1996. The rest of the measurements were obtained from 1997 to 1999 with the exception of sites A60, C31, M07, and M13, which were all obtained in 1999. When possible, these measurements were taken monthly during fall and winter and more frequently during snowmelt.

The reader is cautioned when using the streamflow regression models to estimate response from localized rainfall events; the assumption of a consistent correlation at gaged and ungaged sites is no longer valid because localized rainfall events may have varying effects on streamflow at different sites. Also, it was assumed that streamflow correlations between gaged and ungaged sites were constant from year to year unless there was a change in streamflow caused by an impoundment or diversion. To test this assumption, the relation between streamflow at gaged and ungaged sites was examined at all sampling sites for the entire period of record. Figure 4 shows the variation about the regression line when measured streamflow at ungaged site M27 is related to daily mean streamflow at gaged site M34 for 5 years of record. The majority of streamflow measurements in figure 4, regardless of water year, fall within the 95-percent confidence interval for the regression line. Other sampling sites generally showed little variation in correlation from year to year as well.

Streamflow regression models were derived using ordinary least-squares (OLS) regression with SYSTAT 7.0 software (SPSS Inc., 1997a). Each model was evaluated for significance based on the coefficient of determination (r^2), p values, residual plots, and the standard error of estimate. Values of r^2 less than 0.6 and p values greater than 0.05 were generally considered an indication of a poor correlation. Plots of residuals (where a residual is an estimated value minus its corresponding observed value) related to prediction estimates and time were used to identify the presence of serial correlations. The presence of a serial correlation indicates that sampling bias or a trend may exist in the data set. When data showed evidence of serial correlation, tests were performed to determine if the correlation was due to trend or sampling bias. A combination of parametric and nonparametric tests for trend were used when serial correlations existed. If tests for trends were found to be inconclusive, it was determined that the serially correlated data set was biased and that the data set would not be used to derive a streamflow regression model. References and a brief description of trend testing used for streamflow and water-quality model calibration are described in the following sections. The final parameter, standard error, is an estimate of the standard deviation of the residuals about the regression. The smaller the standard error of estimate, the more representative will be the predictions (Driver and Tasker, 1990). All diagnostics were considered collectively to determine the most appropriate streamflow regression model at ungaged sampling sites.

The form of the regression equation used for estimating streamflow at ungaged sampling sites is:

$$Y_Q = B(X_Q) + \alpha \qquad (1)$$

where

- Y_Q is the streamflow at the ungaged site, in cubic feet per second;
- B is the slope of the regression line;
- X_Q is the streamflow at the gaged site, in cubic feet per second; and
- α is the *y* intercept of the regression line.

In equation 1, the explanatory variable (X_Q) is daily mean streamflow at the gaged site, which is the average streamflow over a 24-hour period. The response variable (Y_Q) estimated using equation 1 is returned as

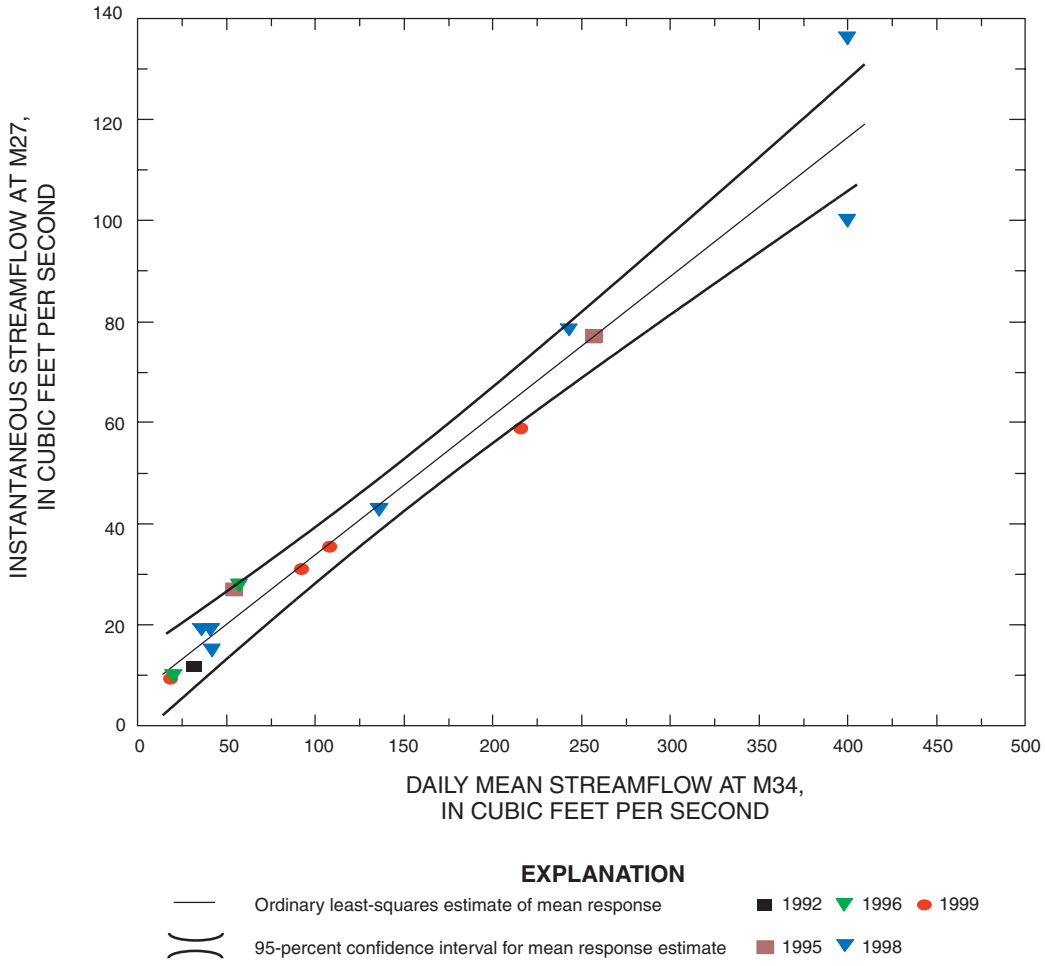

Figure 4. Measured streamflow at ungaged sampling site M27 related to daily mean streamflow at gaged sampling site M34 showing the variation about the regression line of streamflow measurements from differing water years.

an instantaneous streamflow value for the ungaged site of interest because instantaneous streamflow was used to calibrate the models. Because no daily mean streamflow data were available at ungaged sites and because instantaneous streamflow data were not available for all the samples at gaged sites, the instantaneous streamflow value returned by equation 1 is assumed to be similar to the daily mean streamflow. This assumption is based on streamflow regressions between sites A68 and A72, where both instantaneous and daily mean streamflow were used to calibrate the surface-water model at A68. Both the instantaneous and daily mean models tended to underestimate streamflow by an average of about 8–9 percent. However, the mean daily model tended to estimate values that were on average approximately 4 percent lower than those of the instantaneous model.

Water-Quality Regression Models

Water-quality regression models were developed to estimate daily values of hardness and concentrations of dissolved cadmium, copper, and zinc at gaged and ungaged sites. Water-quality data used for regression modeling were obtained during different streamflow regimes at all sampling sites. Constituent concentrations below minimum reporting levels were assigned one-half the value of the minimum reporting level. Alternative methods of dealing with data below minimum reporting levels, such as tobit or logistic regression (Helsel and Hirsch, 1992), are available but were considered beyond the scope of this report and were generally not needed at the majority of sites due to the high levels of trace metals present in the water.

Model Selection

Explanatory variables considered for the regression included streamflow and seasonal terms. A variety of physical and chemical variables such as conductivity, alkalinity, sulfate, and colloidal iron also may help explain variability in a data set (Wetherbee and Kimball, 1989); however, continuous data for these parameters were not available for consideration in this study. A continuous record is needed because estimates of seasonally defined (monthly or multimonthly) loads are generated using daily values as input (explanatory) variables in the regression models. The use of daily values will better define monthly loads as compared to estimates obtained using periodic record from random site visits. Instantaneous values also could be used as input variables; however, some historical data from the streamflow gages used graphic recorders, which store continuous record in analog format, thus making this data extremely difficult to compile and use in electronic format. Therefore, for purposes of consistency, all historical daily values that could be retrieved electronically and compiled easily in spreadsheet form were used in this study.

Derivation of water-quality models at gaged and ungaged sampling sites differed because of the type of streamflow data available at each site. At gaged sampling sites, daily mean streamflow was used to derive the water-quality models because an instantaneous streamflow value was not available for every water-quality sample. At ungaged sites, the regression models were developed from instantaneous streamflow, which was measured at the time of water-quality sampling. As a check for comparability between models derived from daily mean and instantaneous streamflow, zinc and copper data were regressed against the two streamflow types for each gaged site. Results indicated that there was little difference in the slope and intercept of each model; therefore, it was assumed that gaged and ungaged water-quality models were comparable.

In addition to streamflow, the other explanatory variable used for model derivation was a seasonal term. Because solute concentrations tend to follow a hysteretic pattern (fig. 3) in the Animas Basin, it is useful to relate a seasonal component to solute concentration. This relation was established using methods suggested by Aulenbach and Hooper (1994), where sine and cosine pairs are used to simulate constituent concentration as a function of julian date. This approach, however, has limited utility for smaller data sets. Because data sets were small at most of the ungaged sites (7–21 samples), an additional variable was tested in water-quality models. This variable also is based on julian date and is often referred to as a "flushing-dummy variable" (herein referred to as a "flushing variable"). The flushing variable assigns a value of 1 to sample data collected during periods of interest and a value of 0 to the rest, where periods of interest were those associated with outliers observed in the summary statistics. An example plot of outliers is shown in figure 5. Most samples collected at site C20 during the period of April 15–May 31 in any given year (shaded symbols) do not generally follow correlation patterns measured in other months. These outliers were thought to indicate the presence of a hysteretic pattern that could not be completely defined by the existing data set; however, factors driving these processes are not fully understood.

Models were calibrated using interactive-stepwise regression to determine which combination of explanatory variables composed the most suitable regression models (SPSS Inc., 1997b). If too many unnecessary variables are included in a regression model, a decrease in model significance results from lower degrees of freedom (Helsel and Hirsch, 1992). Interactive-stepwise regression allows the user to test different combinations of variables and select the most appropriate model based on diagnostics such as adjusted r^2, standard error of estimate, p values for individual variables, and the F statistic. Following stepwise regression, each model was evaluated for significance using basic statistical diagnostics as evaluation tools. These parameters included r^2, model p values, and residual plots. All diagnostics were considered collectively by using the same guidelines used to evaluate the streamflow regression models.

The utility of a water-quality model typically increases after a data set is linearized. A hyperbolic transformation of streamflow suggested by Johnson and others (1969) was used to linearize the streamflow variable. Transformations are typically performed to improve the linear fit of the data set, where a linear fit of the data will better approximate

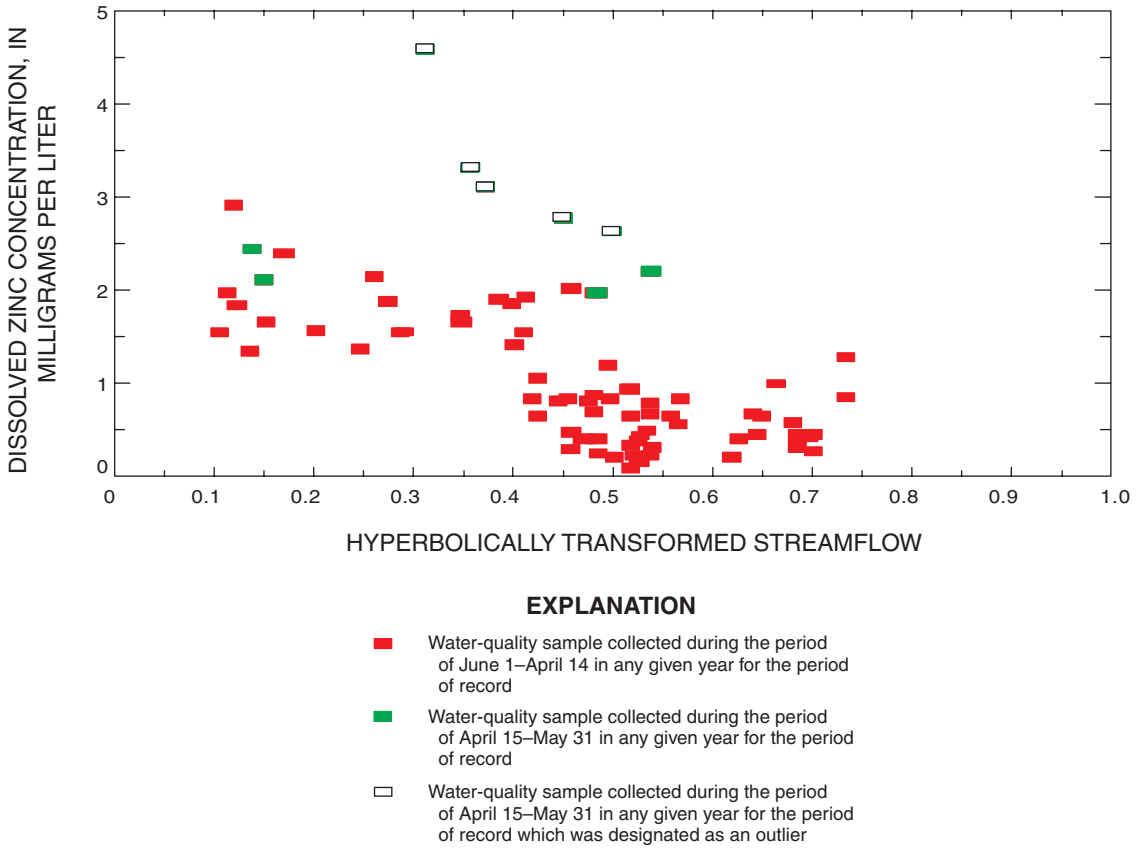

Figure 5. Plot of hyperbolically transformed streamflow related to zinc concentration at site C20 showing the presence of outliers.

the assumption of normality, which is a requirement for parametric statistical techniques like OLS regression. This transformation is defined by the equation:

$$X_h = 1/\{1 + \beta[(X_Q)]\} \qquad (2)$$

where

β is beta, a constant typically in the range 10^{-3} to 10^{2}; and

Q is streamflow, in cubic feet per second.

Beta is fit to linearize a given data set. Prior to the inclusion of other variables, beta was fit visually using a spreadsheet program.

Inverse and logarithmic transformations suggested by Ott (1993) were used to linearize the response variable. Some iteration is required when trying to determine the transformations that would constitute the best regression model. Variable transformations and equation forms for water-quality models are listed in table 5.

When logarithmic transformations are used, a transformation bias is produced when logarithms of the estimated mean response (log of the response variable) are retransformed. This transformation usually results in the underestimation of the estimated mean response. The major portion of this translation bias may be eliminated by multiplying the estimated mean response by a correction factor (Duan, 1983):

$$BCF = 1/n \sum_{i=1}^{n} 10^{e_i}$$

where

BCF is the bias correction factor;

n is the number of observations in the data set; and

e_i is the least-squares residual for observation i from the calibration data set, in log units.

Trend Analysis

If variable transformation did not improve the significance of a given model, a second measure was taken that tests for trend in a given data set. Testing for trend in a data set is useful for determining which data points are representative of the condition of interest. The condition of interest for this report is postremediation (table 1). Trends in a data set also may result from climatic shifts or anthropogenic influences. This study focused on trends that resulted from anthropogenic influences such as impoundments, streamflow diversions, and mined-land remediation. It was assumed the effect of trend resulting from a change in climate would be negligible on the basis of a period of record less than 10 years.

Three techniques were used to evaluate for trends at sampling sites with 30 or more samples. Data sets with fewer than 30 samples generally did not contain sufficient data to establish a representative preremediation sample population. Therefore, it was assumed that trends in data sets at sites with fewer than 30 samples existed if they were downstream from an anthropogenic influence and upstream from a site where a trend was detected.

LOWESS smooth curves were calculated using SYSTAT 7.0 (SPSS Inc., 1997a) software for plots that related time-series data to raw constituent concentrations and residuals. Upward or downward trending LOWESS curves (fig. 6) indicated the presence of a trend in the data set. Next, a parametric test that uses a dummy variable (different from the flushing variable) to indicate the significance of pre- and postcondition samples was used. Pre- and postcondition samples were categorized and assigned a value of 0 or 1 and included as an explanatory variable in a given water-quality model. A trend was detected with this test if the dummy variable was retained in the regression model after stepwise regression at a 5-percent level of significance. The final test was the nonparametric Kolmogorov-Smirnov two-sample test, which compares the cumulative distribution functions for pre- and postcondition residual values (SPSS Inc., 1997b). A trend was detected with this test when the alternative hypothesis (the cumulative distribution functions differ) was accepted at a 5-percent level of significance. An advantage to the Kolmogorov-Smirnov two-sample test is that sample sizes for pre- and postconditions were not required to be equal in size. Note that if no regression models are considered significant for a given constituent after interactive-stepwise regression, no residual-based trend analysis should be performed (Crawford and others, 1983).

Following trend analysis, if it was concluded that a trend existed in a given data, the data set was divided into pre- and postcondition groups and regressions were derived using the postcondition data set.

Table 5. Summary of equation forms used to simulate constituent concentrations at sampling sites

[β, hyperbolic transformation constant; α, the regression coefficient that is the intercept in the regression model; B and B_n, estimated coefficient of explanatory variables in multiple regression; $DV_{1..n}$, flushing variable(s); J_C, first-order julian date transformation; J_D, second-order julian date transformation; J_E, third-order julian date transformation; J_F, fourth-order julian date transformation; X_Q, streamflow in cubic feet per second; X_h, transformed streamflow; C_Q, constituent concentration in milligrams per liter]

Equation form number	Response variable		Explanatory variables		Equation form
	Variable	Transformation	Variable	Transformation	
3	C_Q	None	X_Q	None	$C_Q = B(X_Q) + \alpha$
4	C_Q	Inverse	X_h	Hyperbolic[1]	$1/C_Q = B(X_h) + DV_{1..n}$
			$DV_{1..n}$	None	
5	C_Q	None	X_h	Hyperbolic[1]	$C_Q = B(X_h) + B_1(J_C) + B_2(J_D) + B_3(J_E) + B_4(J_F) + DV_{1..n} + \alpha$
			J_C, J_D, J_E, J_F	Trigonometric[2]	
			$DV_{1..n}$	None	
[3]6	C_Q	Logarithmic	X_h	None	$\log C_Q = B(X_h) + B_1(J_C) + B_2(J_D) + B_3(J_E) + B_4(J_F) + DV_{1..n} + \alpha$
			J_C, J_D, J_E, J_F	Trigonometric[2]	
			$DV_{1..n}$	None	

[1]Hyperbolic transformation is $X_h = 1/\{1+\beta[(X_Q)]\}$.

[2]Trigonometric transformation, first order; $J_C = \sin[(\pi(\text{julian date}))/365]$, second order; $J_D = \text{cosine}[(\pi(\text{julian date}))/365]$, third order; $J_E = \sin[(\pi(\text{julian date}))/182.5]$, fourth order; $J_F = \text{cosine}[(\pi(\text{julian date}))/182.5]$.

[3]Equation form uses a logarithmic transformation that requires a bias correction factor when estimating mean response.

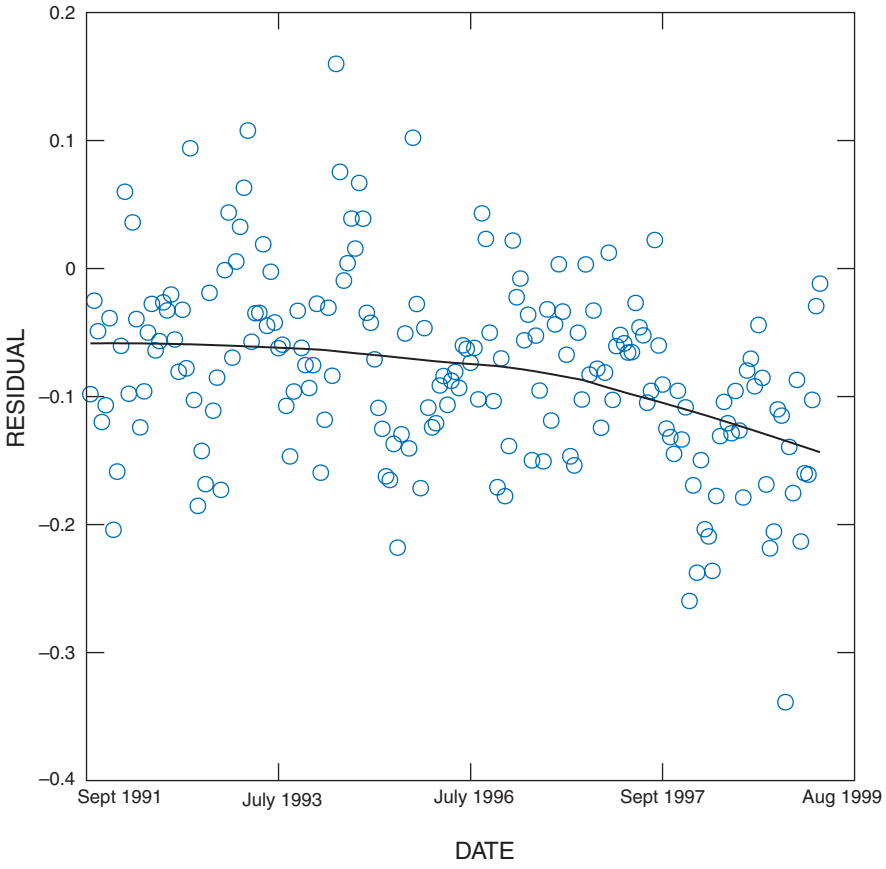

Figure 6. Residuals scatterplot and LOWESS smooth line showing a downward trend in dissolved zinc concentration at site M34.

An example of how a water-quality model is derived for zinc at site C18 using the aforementioned methods is given in figure 7. Graph A shows streamflow related to measured zinc concentration. Regression diagnostics and graph A indicate that the data may benefit from a hyperbolic transformation of streamflow or additional explanatory variables, or both. Graph B shows how a hyperbolic transformation of streamflow helps to linearize the data set. To test for hysteresis in the data set, the additional explanatory variables related to date (sin cosine pairs and the dummy variable) are added to the model (graph C). After stepwise regression, an evaluation of regression diagnostics indicated that model significance had improved. Trend testing was then done using the model, and residuals from the model and results indicated no trend was detectable. Concentrations estimated from the model are checked in graph D, which illustrates an approximate 1 to 1 relation (slope 0.95) and residuals variance (data scatter about the 1 to 1 line) of 0.89 mg/L between estimated zinc related to measured zinc. Deviation in the 1:1 line in figure 7D is thought to have arisen from some logistical problems encountered while collecting winter samples (typically higher concentration samples) at alternate sites than summer samples because of avalanche danger. This deviation was not observed at other sites.

Water-Quality Profiles

Using the streamflow and water-quality regression models, water-quality profiles were calculated for the 15 sampling sites. Profiles depicting seasonal fluctuations in streamflow, constituent concentration, and constituent load were calculated. Streamflow profiles were developed by first quantifying daily mean streamflow at each sampling site. At ungaged sites, the streamflow regression models were used to

estimate daily mean streamflows, and at gaged sites, the continuous streamflow record was used. The daily mean streamflows were used to calculate mean monthly flows that were then plotted as streamflow profiles by subbasin. Daily mean streamflow values were used in the water-quality models to estimate daily mean constituent concentration. The daily mean constituent concentrations were used to calculate averaged monthly concentrations and results were then plotted at each sampling site as a concentration profile. Daily mean constituent loads were calculated from the product of the daily mean constituent concentration and daily mean streamflow. The resulting loads were then averaged to produce mean-monthly loads which were plotted as loading profiles. Concentration and loading profiles were not developed at sites where water-quality regression models were not statistically significant ($p > 0.05$).

Limitations of Data Analysis

Use of the statistical regression models provided in this report requires the adherence to specific guidelines and an understanding of the limitations inherent in each model. Estimates from streamflow and water-quality regression models in this report were only provided after careful consideration of the following guidelines and limitations:

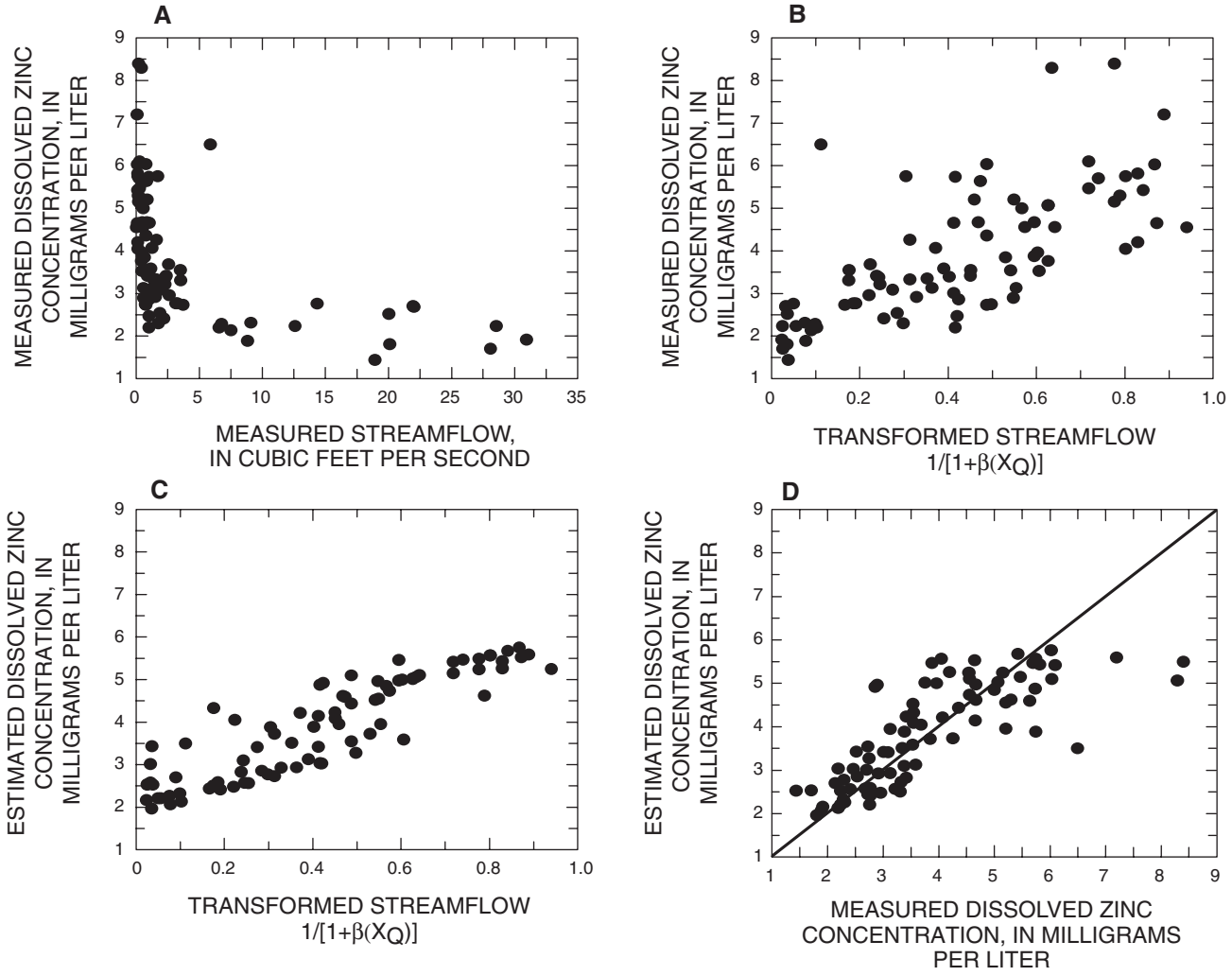

Figure 7. Zinc concentration graphs at sampling site C18 that relate: (A) Measured streamflow to measured zinc concentration, (B) hyperbolically transformed streamflow to measured zinc concentration, (C) hyperbolically transformed streamflow to estimated zinc concentration, and (D) estimated zinc to measured zinc concentration.

1. Models are site specific.
2. Models with considerable standard error values are less accurate than models having low values for standard error.
3. Model output represents water-quality conditions during the period sampled and do not necessarily represent past or future conditions.
4. Models represent a specific range of estimations which, when exceeded, may decrease a model's usefulness.
5. Negative values returned by a water-quality model can occur at the extremes of the estimation range if a model's calibration data set contains extensive data below a constituent's minimum reporting level (MRL). Loading values for negative concentration estimates were reported as one-half the value of the minimum estimate in one annual cycle.
6. Model verification (using sample data collected but not included in model derivations) was done at sites M27 and M34 only for September because of the availability of data at the time this report was written (2000).

Although the correlation for gaged and ungaged streamflow is assumed to be constant (fig. 4) for the period of record, values estimated using the streamflow regression models will not always fall within a model's standard error. This situation can occur under certain environmental conditions or if the range of estimation is not considered. Because snow depth, snowpack temperature, and rainfall can vary in a basin with varying elevation, aspect, and vegetation cover, the onset of runoff from these zones will vary (Dunne and Leopold, 1978). This is especially true when estimating streamflow at ungaged sites during periods of intense localized rainfall because one or more of the ungaged subbasins may not experience any rainfall runoff from a rainfall that has affected streamflow at a gaged site. When this occurs, the statistical correlation between gaged and ungaged sites is no longer meaningful. Caution should be used when estimating streamflow at ungaged sites during rainfall. The authors were aware of this problem and therefore chose to report only monthly loads, thus avoiding possibly sizable errors that may result from estimating daily loads during the rainy season. Also, the timing of snowmelt runoff (lag time) will differ at each ungaged sampling site because snowpack at higher elevations or on northern aspects is usually the last to melt and south-facing, low-elevation basins will melt early. Estimates made for ungaged sites using the water-quality models could not be adjusted to account for differences in timing of snowmelt runoff because continuous streamflow data were not available.

SEASONALITY OF WATER QUALITY IN THE UPPER ANIMAS RIVER BASIN

This section contains a summary and analysis of seasonal variations in water quality in Cement Creek, Mineral Creek, and the upper Animas River using methods described previously for constructing water-quality profiles. The summary lists some basic statistics that describe the range of water quality in the Animas Basin data set and also gives a brief account of where and for which constituents water-quality trends are present, as well as what factors may have initiated these trends. The analysis contains concentration and loading profiles for hardness and dissolved cadmium, copper, and zinc at all locations where water-quality models were significant. Coefficients and equation forms for streamflow and water-quality models are provided.

Water-Quality Summary Statistics

A summary of water-quality and streamflow data for each sampling site (fig. 1) is presented in table 6. Minimum, maximum, median, and mean values for dissolved cadmium, dissolved copper, dissolved zinc, and hardness were calculated for each site. Also included are the results of water-quality trend analysis at sites with 30 or more water-quality samples. Trend analysis is important for determining which portion of a water-quality data set is representative of current conditions. If a water-quality trend was detected, the direction of trend also is given as upward (U) or downward (D). Where no trend was detected, it is assumed that no trend exists; however, subtle changes in stream chemistry over time may not be detectable using the methods described in this report.

Table 6. Summary statistics for selected constituents and properties at sampling sites

[MRL, minimum reporting level; ft^3/s, cubic feet per second; mg/L, milligrams per liter; D, downward trend detected; U, upward trend detected; nm, no significant model; no, no trend detected]

Summary statistic	Streamflow (ft^3/s)	Cadmium, dissolved (mg/L)	Copper, dissolved (mg/L)	Zinc, dissolved (mg/L)	Hardness as $CaCO_3$ (mg/L)
Cement Creek at Gladstone (C18)					
Number of samples	47	84	84	85	86
Minimum	0.05	MRL	0.020	1.44	37.0
Maximum	30.9	0.120	3.190	8.40	327
Median	1.04	0.012	0.340	3.53	150
Mean	3.99	0.015	0.396	3.84	167
Trend	no	no	no	no	no
Cement Creek near Gladstone (C20)					
Number of samples	47	85	85	85	85
Minimum	1.5	MRL	MRL	MRL	151
Maximum	32.6	0.100	0.970	4.58	1,660
Median	3.76	0.003	0.010	0.82	981
Mean	6.87	0.006	0.090	1.11	899
Trend	D	nm	nm	no	D
Cement Creek near Fairview Gulch (C31)					
Number of samples	13	13	13	13	13
Minimum	7.23	MRL	0.020	0.870	75.4
Maximum	98	0.016	0.260	1.75	538
Median	22.9	0.006	0.150	1.18	224
Mean	33.1	0.008	0.130	1.15	286
Cement Creek near Yukon Mine (C43)					
Number of samples	9	7	7	9	7
Minimum	20.2	MRL	0.08	0.768	124
Maximum	95.5	0.130	0.186	1.20	486
Median	28.2	0.004	0.114	0.926	182
Mean	43.0	0.006	0.121	0.946	235
Cement Creek at Silverton (C48)					
Number of samples	82	170	170	166	113
Minimum	12.4	MRL	MRL	0.462	16
Maximum	329	0.011	0.250	1.57	1,460
Median	32.3	0.003	0.055	0.738	291
Mean	57.9	0.002	0.063	0.768	319
Trend	no	nm	nm	nm	D
Mineral Creek near Headwaters (M02)					
Number of samples	18	18	18	18	17
Minimum	0.02	MRL	1.91	7.84	70
Maximum	2.08	1.12	82.0	230	423
Median	0.12	0.256	2.92	80.0	244
Mean	0.46	0.353	2.96	85.3	239
Mineral Creek at Chattanooga (M07)					
Number of samples	17	17	17	17	16
Minimum	0.17	MRL	0.020	0.180	24.5
Maximum	65.5	0.028	1.90	8.90	120
Median	11.8	0.005	0.299	1.39	42.2
Mean	20.2	0.008	0.537	2.41	50.4

Table 6. Summary statistics for selected constituents and properties at sampling sites—Continued

[MRL, minimum reporting level; ft^3/s, cubic feet per second; mg/L, milligrams per liter; D, downward trend detected; U, upward trend detected; nm, no significant model; no, no trend detected]

Summary statistic	Streamflow (ft^3/s)	Cadmium, dissolved (mg/L)	Copper, dissolved (mg/L)	Zinc, dissolved (mg/L)	Hardness as $CaCO_3$ (mg/L)
Mineral Creek at Burro Bridge (M13)					
Number of samples	18	18	18	18	14
Minimum	3.48	MRL	0.020	0.210	26.1
Maximum	123	0.006	0.220	1.80	318
Median	26.8	0.003	0.058	0.719	99.2
Mean	39.1	0.003	0.075	0.868	120
Mineral Creek upstream from South Fork Mineral Creek (M27)					
Number of samples	16	21	21	21	14
Minimum	9.09	MRL	0.013	0.181	59.9
Maximum	134	0.010	0.190	1.50	446
Median	27.5	0.002	0.056	0.605	156
Mean	47.8	0.002	0.069	0.589	188
Mineral Creek at Silverton (M34)					
Number of samples	207	207	207	207	207
Minimum	14.8	MRL	MRL	0.070	45.2
Maximum	863	0.002	0.137	0.750	341
Median	77.0	0.001	0.011	0.234	150
Mean	157	0.001	0.021	0.265	150
Trend	no	no	D	D	no
Animas River at Eureka (A33)					
Number of samples	17	17	17	17	17
Minimum	1.16	0.002	MRL	0.260	30.4
Maximum	177	0.003	0.032	0.573	133
Median	16.6	0.002	0.011	0.458	53.9
Mean	44.6	0.002	0.014	0.442	63.8
Animas River at Howardsville (A53)					
Number of samples	17	17	17	17	17
Minimum	14.3	0.001	MRL	0.197	47.7
Maximum	505	0.002	0.010	0.366	149
Median	73.9	0.001	0.002	0.270	92.0
Mean	140	0.001	0.003	0.267	92.2
Animas River near Arrastra Gulch (A60)					
Number of samples	11	11	11	11	11
Minimum	26.2	0.001	MRL	0.059	47.5
Maximum	591	0.001	0.015	0.320	138
Median	166	0.001	0.002	0.230	72.2
Mean	182	0.001	0.004	0.246	85.3
Animas River at Silverton (A68)					
Number of samples	70	70	70	70	66
Minimum	8.48	0.008	MRL	0.226	20.0
Maximum	883	0.033	0.023	1.24	192
Median	176	0.001	0.005	0.378	80.0
Mean	234	0.002	0.006	0.456	70.0
Trend	no	no	no	no	no

Table 6. Summary statistics for selected constituents and properties at sampling sites—Continued

[MRL, minimum reporting level; ft^3/s, cubic feet per second; mg/L, milligrams per liter; D, downward trend detected; U, upward trend detected; nm, no significant model; no, no trend detected]

Summary statistic	Streamflow (ft^3/s)	Cadmium, dissolved (mg/L)	Copper, dissolved (mg/L)	Zinc, dissolved (mg/L)	Hardness as $CaCO_3$ (mg/L)
Animas River downstream from Silverton (A72)					
Number of samples	114	114	114	114	106
Minimum	55.5	MRL	MRL	0.160	39.0
Maximum	2,100	0.005	0.029	0.940	340
Median	266	0.001	0.006	0.400	134
Mean	501	0.002	0.007	0.430	146
Trend	no	no	no	no	no

Dissolved cadmium concentrations ranged from the minimum reporting level (MRL) to 1.12 mg/L (M02). Mean cadmium concentrations were highest (0.353 mg/L) at site M02 and lowest (0.001 mg/L) at sites M34, A53, and A60. Dissolved copper concentrations ranged from the MRL to 82.0 mg/L (M02). Mean copper concentrations were highest (2.96 mg/L) at site M02 and lowest (0.003 mg/L) at site A53. Dissolved zinc concentrations at sampling sites ranged from the MRL to 230 mg/L (M02). Mean zinc concentration levels were highest (85.3 mg/L) at site M02 and lowest (0.246 mg/L) at site A60. The only site with zinc concentrations less than the MRL was site C20. Hardness concentrations ranged from 16.0 mg/L (C48) to 1,660 mg/L (C20). Mean hardness concentrations were highest at site C20 (899 mg/L) and lowest at site M07 (50.4 mg/L).

Measured streamflow at the sampling sites ranged from 0.02 ft^3/s at site M02 to 2,100 ft^3/s at site A72. Mean streamflow at the farthest downstream sampling site (A72) was 501 ft^3/s and median streamflow was 266 ft^3/s.

Water-Quality Profiles

Streamflow regression model coefficients for each ungaged site are listed in table 7. Each streamflow model uses equation 1 ("Streamflow Regression Models" section). Water-quality regression model coefficients and the appropriate equation form number from table 5 are listed in table 8. All streamflow and water-quality regression models used to estimate water-quality profiles were significant at the 5-percent level ($p < 0.05$) and generally showed constant variance throughout the range of prediction in residual plots. Water-quality regression models were not considered significant enough for estimation for cadmium and copper at all sampling sites in Cement Creek subbasin and for zinc at sites C31, C43, and C48.

The range of estimation provided for each site in tables 7 and 8 refers to the range of streamflow at the time samples were collected. Estimates made using the streamflow and water-quality regression models outside the range of estimation may be less reliable than those made within the limits of model calibration.

Water-quality profiles for selected months (February, May, June, July, and September) were plotted to illustrate seasonal increases or decreases in concentration and load between sampling sites in an average year. February was selected to represent base flow; May, June, and July were selected to represent snowmelt runoff (spring and summer); and September was selected to represent the monsoonal season (late summer and fall). Note that the following sections use the monthly means (figs. 10, 13, and 16) for May, June, and July to represent snowmelt runoff, while the base flow and monsoonal periods (February and September, respectively) use only one monthly mean each from the water-quality profiles. This was done to account for the extreme variability in water quality during the runoff period.

Table 7. Summary of streamflow regression model coefficients and diagnostics at ungaged sampling sites

[α, the regression coefficient that is the intercept in the regression model; r^2, the coefficient of determination; X_Q, explanatory variable streamflow, in cubic feet per second, at streamflow-gaging station]

Sampling site (fig. 1)	Range of estimation[1] (ft^3/s)	α	Coefficients for explanatory variable X_Q (ft^3/s)	r^2	Standard error of estimate (ft^3/s)
			Cement Creek[2]		
C18	8.5–239	–1.26	0.15	0.75	3.5
C20	8.5–202	–1.14	0.206	0.87	2.35
C31	12–174	–2.41	0.53	0.98	4.4
C43	17–123	–0.12	0.76	0.99	2.23
			Mineral Creek[3]		
M02	19–903	0.0	0.002	0.83	0.27
M07	19–550	0.0	0.099	0.84	8.3
M13	32–550	0.0	0.21	0.94	8.8
M27	19–400	6.13	0.28	0.96	7.8
			Upper Animas River[4]		
A33	57–1,500	–7.4	0.12	0.96	10.7
A53	57–1,500	0.0	0.35	0.95	31.3
A60	83–1,500	0.0	0.40	0.94	40.7
A68	56–2,040	0.0	0.42	0.99	24.2

[1]Estimation range applies to the explanatory variable of streamflow (X_Q) from corresponding streamflow-gaging station.
[2]The explanatory variable (X_Q) is obtained from streamflow-gaging station number 09358550.
[3]The explanatory variable (X_Q) is obtained from streamflow-gaging station number 09359010.
[4]The explanatory variable (X_Q) is obtained from streamflow-gaging station number 09359020.

Cement Creek

Estimates of seasonal water quality in Cement Creek subbasin were calculated for sites C18, C20, C31, C43, and C48. Regression models were statistically significant for streamflow and hardness at all sampling sites. Models at two sites (C18 and C20) were statistically significant for zinc, whereas no models were significant for cadmium and copper at any sites in Cement Creek. Significant models for hardness and zinc had r^2 values ranging from 0.61 to 0.95.

The streamflow profile for sites in Cement Creek is shown in figure 8. The profile indicates that base flow in Cement Creek ranged among sampling sites from less than 1.0 ft^3/s at C18 to about 13 ft^3/s at C48. Peak snowmelt runoff generally occurs in June and ranged from about 24 ft^3/s at site C18 to 150 ft^3/s at C48. Estimated streamflow at the mouth of Cement Creek subbasin (C48) is generally about 10 to 22 percent of the total streamflow at the mouth of the Animas Basin (A72) for any given month. About 30 to 40 percent of the streamflow at site C48 originates between sites C20 and C31 during snowmelt runoff. Average annual streamflow at C48 is about 42 ft^3/s, or a yield of about 2.1 $ft^3/s/mi^2$ (cfsm) from the Cement Creek subbasin.

A trend was detected at site C20 that indicated that a decrease in streamflow occurred in 1996. This change may have resulted from the September 1996 closure of the American Tunnel bulkhead near Gladstone, Colo. The trend was most apparent during base-flow conditions (fig. 9). A trend during high flow was not apparent, possibly due to streamflow measurement error, which can be more prevalent during high stage. No trends in streamflow were detected at C48; therefore, all streamflow measurements were utilized in streamflow model development at sites C31 and C43. Data for samples collected before September 1996, however, were not used to derive models at site C20.

Table 8. Summary of water-quality regression model coefficients and diagnostics at all 15 sampling sites

[β, constant used in hyperbolic transformation; α, the regression coefficient that is the intercept in the regression model; B and B_n, coefficient of explanatory variables in multiple regression; DV_1, dummy variable; J_C, first-order julian date transformation; J_D, second-order julian date transformation; J_E, third-order julian date transformation; J_F, fourth-order julian date transformation; X_Q, streamflow in cubic feet per second; X_h, transformed streamflow; r^2, the coefficient of determination; --, indicates explanatory variable was not used in the regression model or was not applicable]

Sampling site	Equation form from table 5	Range of estimation (ft^3/s)	β	α	B..B_n								Standard error of estimate (mg/L)	Bias correction factor
					X_Q (ft^3/s)	X_h	J_C	J_D	J_E	J_F	DV_1	r^2		
Hardness—Cement Creek														
C18	5	0.047–32	0.55	43.3	--	171	--	--	--	--	[c]93.9	0.82	36.7	--
C20	5	1.5–35.3	10	154	--	19,429	--	--	--	--	--	0.90	120	--
C31	5	7.2–98.0	1	46.1	--	4,485	--	--	--	--	--	0.95	40.3	--
C43	5	12.6–95.5	0.1	30.6	--	900.5	--	--	--	--	--	0.91	43.2	--
C48	5	12.0–329	10	64.8	--	62,397	--	--	--	--	--	0.91	49.4	--
Dissolved zinc—Cement Creek														
C18	5	0.047–32	1.33	2.55	--	2.86	0.32	0.65	--	--	[b]0.62	0.61	0.95	--
C20	5	1.5–35.3	0.24	1.66	--	–1.39	0.061	–0.40	--	--	[a]1.44	0.73	0.538	--
Dissolved cadmium—Mineral Creek														
M02	5	0.02–2.1	100	0.0	--	2.23	--	--	--	--	--	0.92	0.115	--
M07	5	0.17–65.5	0.41	0.0	--	0.03	--	--	--	--	--	0.90	0.002	--
M13	5	3.5–123	0.05	0.0	--	0.0071	--	--	--	--	--	0.95	0.001	--
M27	5	9.1–134	0.07	0.0007	--	0.0041	--	--	--	--	--	0.64	0.0005	--
M34	5	15–863	0.019	0.0005	--	0.0012	0.0003	0.0000	0.0001	-0.0002	--	0.65	0.0003	--
Dissolved copper—Mineral Creek														
M02	5	0.02–2.1	10	–1.07	--	60.4	--	--	--	--	--	0.93	5.25	--
M07	5	17–65.5	0.50	0.0	--	1.19	--	--	--	--	--	0.81	0.095	--
M13	5	3.5–123	1.0	0.020	--	0.452	--	--	--	--	--	0.78	0.018	--
M27	5	9.1–134	0.05	–0.002	--	0.173	--	--	--	--	--	0.80	0.019	--
M34	5	15–964	0.05	–0.005	--	0.087	0.0096	0.0002	--	--	--	0.76	0.01	--
Hardness—Mineral Creek														
M02	5	0.02–2.1	10	75.9	--	382.7	--	--	--	--	--	0.80	60.3	--
M07	5	17–65.5	0.31	23.05	--	59.4	--	--	--	--	--	0.92	5.5	--
M13	5	3.5–123	1.5	37.7	--	1,552	--	--	--	--	--	0.91	25.5	--
M27	5	9.1–134	1.1	34.3	--	4,196	--	--	--	--	--	0.94	32.6	--
M34	5	15–752	0.05	38.9	--	417	--	--	--	--	--	0.95	17.0	--
Dissolved zinc—Mineral Creek														
M02	5	0.02–2.1	12	0.0	--	176	--	--	--	--	--	0.98	4.06	--
M07	5	17–65.5	0.25	–0.014	--	4.44	--	--	--	--	--	0.98	0.15	--
M13	5	3.5–123	0.07	0.005	--	1.88	--	--	--	--	--	0.94	0.120	--
M27	5	9.1–134	0.04	0.038	--	0.985	--	--	--	--	--	0.91	0.070	--
M34	5	15–863	0.025	0.078	--	0.510	0.049	0.037	–0.024	–0.038	--	0.91	0.051	--

Table 8. Summary of water-quality regression model coefficients and diagnostics at all 15 sampling sites—Continued

[β, constant used in hyperbolic transformation; α, the regression coefficient that is the intercept in the regression model; B and B_n, coefficient of explanatory variables in multiple regression; DV_1, dummy variable; J_C, first-order julian date transformation; J_D, second-order julian date transformation; J_E, third-order julian date transformation; J_F, fourth-order julian date transformation; X_Q, streamflow in cubic feet per second; X_h, transformed streamflow; r^2, the coefficient of determination; --, indicates explanatory variable was not used in the regression model or was not applicable]

Sampling site	Equation form from table 5	Range of estimation (ft^3/s)	β	α	B..B_n								Standard error of estimate (mg/L)	Bias correction factor
					X_Q (ft^3/s)	X_h	J_C	J_D	J_E	J_F	DV_1	r^2		
Dissolved cadmium—Upper Animas River														
A33	5	1.15–177	0.005	0.0	--	0.0026	--	--	--	--	--	0.95	0.0005	--
A53	3	14.3–505	--	0.0007	2.36–E6	--	--	--	--	--	--	0.66	0.0003	--
A60	4	26.2–680	100	1089	--	505,000	--	--	--	--	[f]–310	0.60	0.006	--
A68	6	8.5–880	0.004	–3.34	--	0.822	0.064	–0.009	--	--	[f]0.147	0.64	0.0014	1.0
A72	5	55.5–2340	0.004	0.001	--	0.0013	0.00048	0.00005	–0.00006	–0.0002	[b]0.0003	0.74	0.0003	--
Dissolved copper—Upper Animas River														
A33	5	1.15–177	0.2	0.0051	--	0.01711	0.0062	–0.0015	--	--	[d]0.017	0.83	0.005	--
A53	5	14.3–505	0.01	0.0	--	0.0032	--	--	--	--	[f]0.005	0.88	0.0015	--
A60	5	26.2–680	0.000001	–28.42	--	28.42	–0.0011	–0.0061	--	--	[f]0.015	0.92	0.0019	--
A68	5	8.5–880	--	0.003	--	--	0.001	–0.0003	–0.001	–0.0001	[b]0.0033	0.62	0.002	--
A72	5	55.5–2340	--	0.011	--	--	0.0075	0.0057	0.0028	–0.00126	--	0.80	0.003	--
Hardness—Upper Animas River														
A33	5	1.15–177	0.1	57.2	--	49.3	–0.187	21.0	13.0	–1.34	--	0.98	4.6	--
A53	5	14.3–505	0.01	27.2	--	122	--	--	--	--	--	0.95	6.6	--
A60	5	26.2–680	0.0078	23.3	--	122	--	--	--	--	--	0.91	9.0	--
A68	5	8.5–880	0.013	45.1	--	144	7.24	10.0	--	--	--	0.97	8.0	--
A72	5	55.5–2,340	0.02	48.8	--	520	8.77	9.61	–1.22	–6.58	--	0.93	23.2	--
Dissolved zinc—Upper Animas River														
A33	5	1.15–177	0.035	0.307	--	0.253	--	--	--	--	--	0.65	0.051	--
A53	5	14.3–505	0.0009	0.0	--	0.291	--	--	--	--	[d]0.042	0.98	0.038	--
A60	5	26.2–680	0.002	0.0	--	0.303	--	--	--	--	[f]0.076	0.97	0.044	--
A68	5	8.5–1,050	0.007	0.0	--	0.834	0.188	–0.028	--	--	[e]0.140	0.90	0.188	--
A72	5	55.5–2,340	0.01	0.249	--	0.598	0.152	0.0298	–0.0267	–0.0592	--	0.87	0.07	--

[a]A value of 1 is assigned to the flushing variable during the period April 15 to May 31.
[b]A value of 1 is assigned to the flushing variable during the period April 1 to May 31.
[c]A value of 1 is assigned to the flushing variable during the period January 1 to March 31.
[d]A value of 1 is assigned to the flushing variable during the period May 1 to May 31.
[e]A value of 1 is assigned to the flushing variable during the period April 1 to June 30.
[f]A value of 1 is assigned to the flushing variable during the period May 1 to June 30.

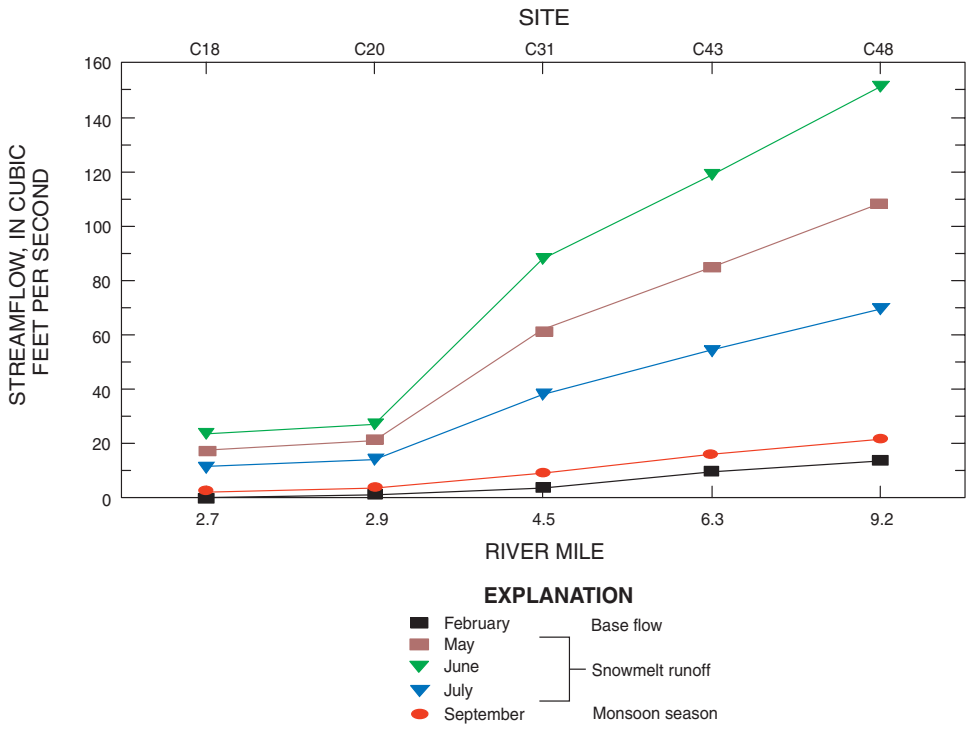

Figure 8. Streamflow profile for Cement Creek subbasin.

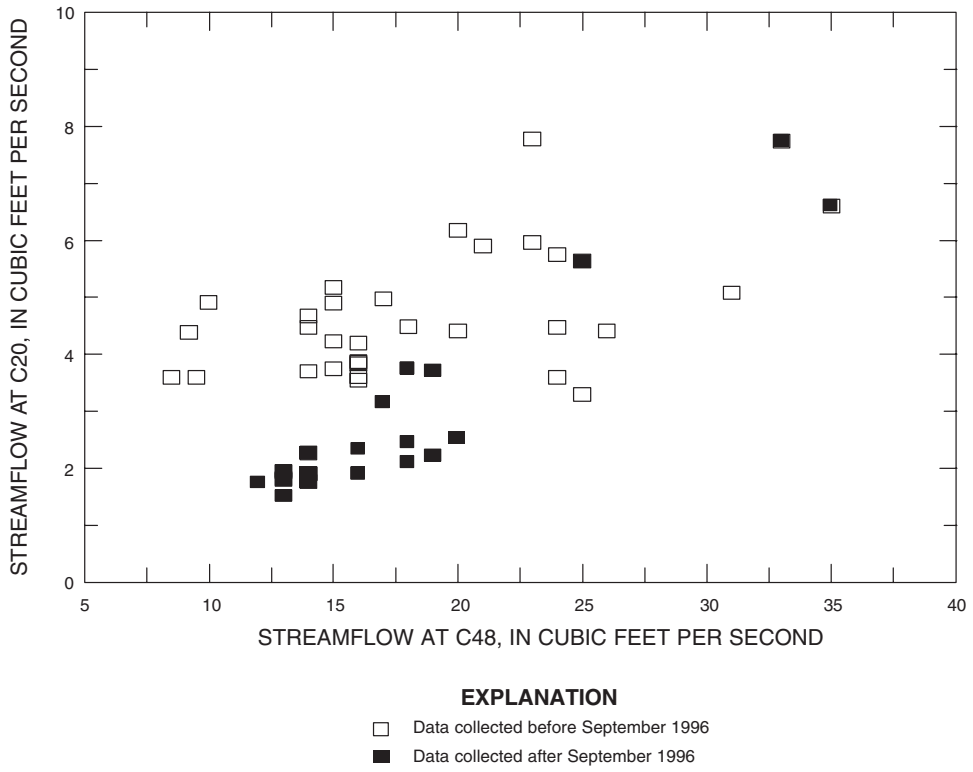

Figure 9. Streamflow data before and after the American Tunnel bulkhead closure in September of 1996.

Concentration and loading profiles for hardness and zinc estimated using the Cement Creek water-quality models are shown in figure 10. The highest monthly concentration of hardness (1,275 mg/L) was estimated at site C20 during base flow and the lowest (55 mg/L) was estimated at site C18 during snowmelt runoff. The largest increases in hardness concentration were estimated between sites C18 and C20 throughout the year, with an average increase during base flow of about 1,000 mg/L and an increase during snowmelt runoff of about 130 mg/L. Hardness concentrations in Cement Creek were lowest at site C18 and highest at site C20 year-round.

The largest hardness load in Cement Creek was estimated at site C48 during snowmelt runoff (87,000 lb/d), and the smallest was estimated at site C18 during base flow (1,000 lb/d). Among the sites, the largest increase in hardness load to Cement Creek during base flow occurred between sites C18 and C20 (about 10,000 lb/d); however, loading between sites was fairly consistent regardless of location at this time. During snowmelt runoff, the largest increase in hardness loading to Cement Creek also occurred between sites C18 and C20 (about 29,300 lb/d).

A flushing variable was retained in the hardness water-quality model after stepwise regression at site C18 for the period of January 1 to March 31 (DV, table 8). When estimating concentrations at this site during this period, a value of 1 is assigned to the flushing variable. The reason for the increase in hardness concentration during this period is not known, but outliers were apparent in XY plots of the measured sample data much like the outliers for zinc were apparent at C20 (fig. 5).

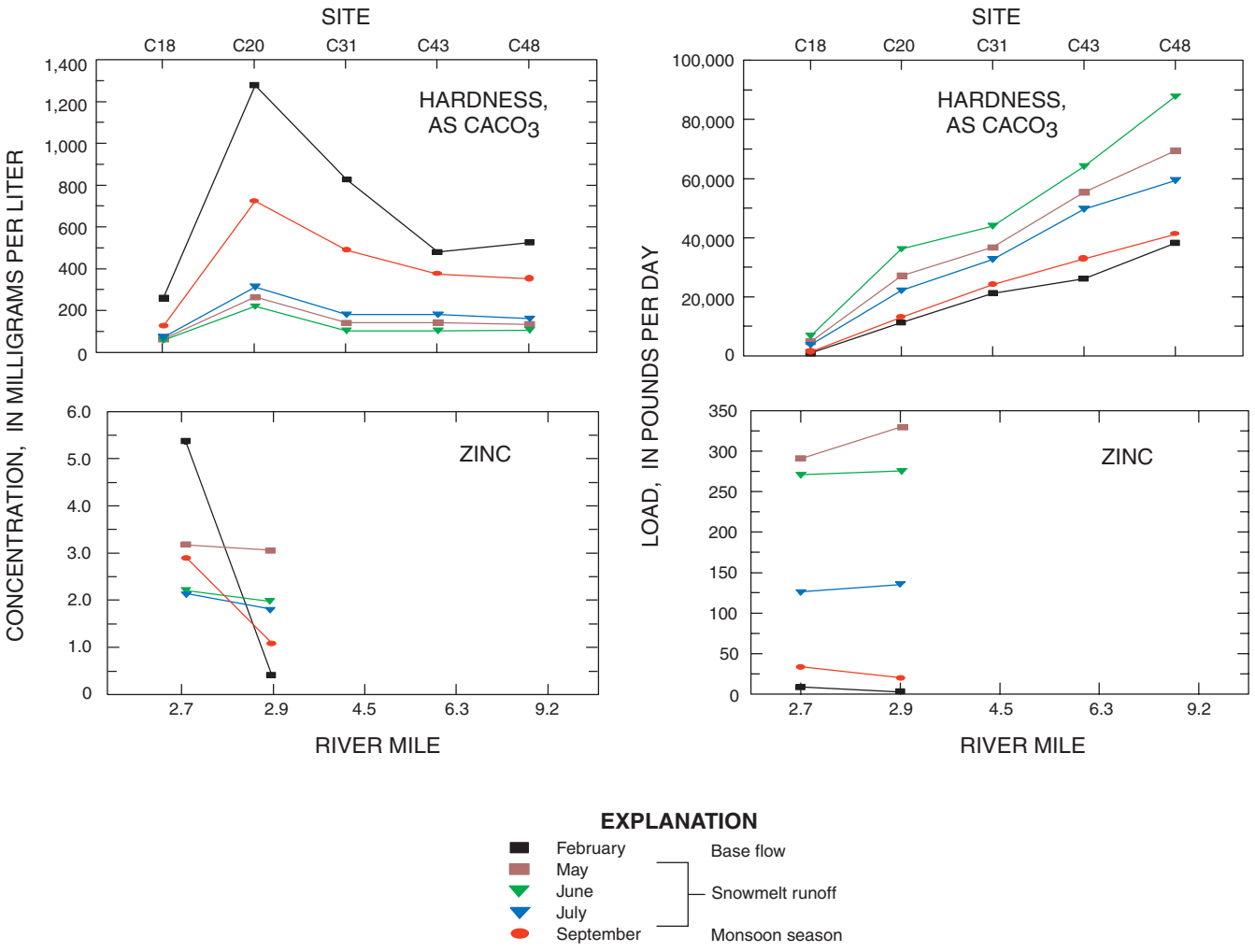

Figure 10. Water-quality profiles for hardness and dissolved zinc at Cement Creek sampling sites.

A downward trend in hardness concentration was detected at sites C20 and C48. This trend correlates to the period when the American Tunnel bulkhead was closed in September of 1996 (table 1). Figure 11 shows the apparent shift in the correlation of streamflow with hardness concentration that occurred during this time period. As a result of trend detection, data collected before September 1996 were not used to derive water-quality regression models for hardness at sites C20, C31, C43, and C48.

The highest monthly concentration of zinc (5.4 mg/L) was estimated at site C18 during base flow and the lowest (0.40 mg/L) was estimated at site C20 during the same period (fig. 10). Concentrations at site C18 were higher during base flow than snowmelt runoff, but concentrations at site C20 tended to be lower during base flow relative to snowmelt runoff concentrations. This may be a result of the water-treatment plant located between sites C18 and C20; the plant treats most of the water in Cement Creek during the base flow (winter) but does not have the capacity to treat all the streamflow during snowmelt runoff. Both sampling sites retained a flushing variable for either April through May or May (DV, table 8).

The largest and smallest monthly loads of zinc were estimated at site C20 during May (330 lb/d) and February (2.4 lb/d). The largest increase in zinc loading between the two sites occurred in May (about 50 lb/d); however, this amount is small relative to the loading that occurred upstream from C20, which ranged from 90 to 100 percent (depending on the season) of the total load at C20.

Mineral Creek

Streamflow and water-quality profiles in Mineral Creek subbasin were calculated for sites M02, M07, M13, M27, and M34. Regression models at all sites in Mineral Creek were statistically significant for streamflow, hardness, cadmium, copper, and zinc and had r^2 values ranging from 0.64 to 0.98 (table 8). The

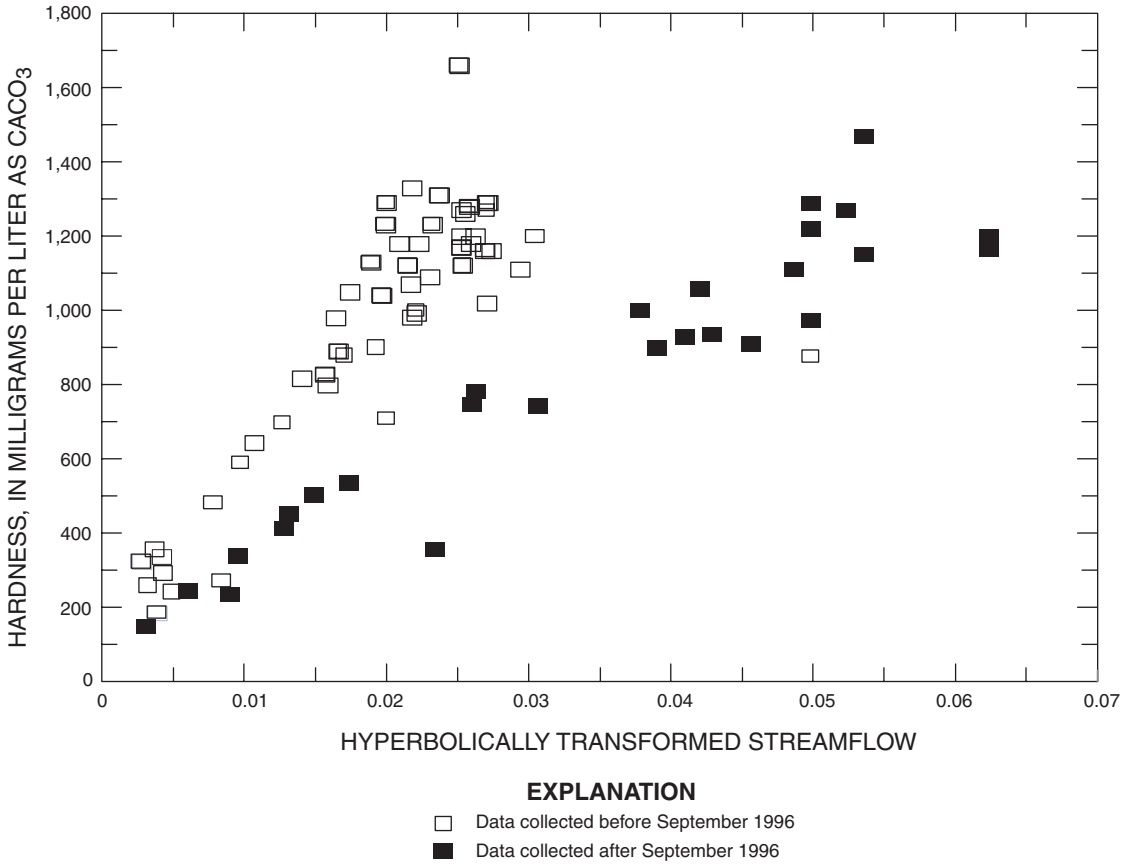

Figure 11. Hardness data at site C20 before and after the American Tunnel bulkhead closure in September of 1996.

streamflow profile for Mineral Creek subbasin is shown in figure 12, and concentration and loading profiles for hardness and metals are shown in figure 13.

The streamflow profile for Mineral Creek indicates that base flow ranged from less than 0.1 ft^3/s at M02 to about 21 ft^3/s at M34. Peak snowmelt runoff generally occurs in June and ranges from about 1.0 ft^3/s at site M02 to 460 ft^3/s at M34. Streamflow at the mouth of Mineral Creek (M34) accounts for about 32 to 52 percent of the total streamflow at A72, of which about 43–70 percent originates between sites M27 and M34. Average annual streamflow draining Mineral Creek subbasin is about 120 ft^3/s or 2.2 cfsm.

The highest monthly concentration of hardness (335 mg/L) was estimated at site M02 during February, and the lowest (26 mg/L) was estimated at site M07 in June. Hardness values were highest at site M02 throughout the year with concentrations that ranged from 100 to 335 mg/L; however, concentrations at site M27 approached 335 mg/L during base flow.

The largest monthly hardness load in Mineral Creek was estimated at site M34 during June (139,000 lb/d), and the smallest was estimated at site M02 in February (86 lb/d). The largest increase in hardness loading to Mineral Creek during base flow occurred between sites M13 and M27 (16,500 lb/d), and the largest increase in loading during snowmelt runoff occurred between sites M27 and M34 (71,000 lb/d). Hardness loads from Mineral Creek are generally about 27 to 37 percent of the hardness load at A72 for any given month.

The highest monthly concentration of cadmium (0.39 mg/L) was estimated at site M02 in February, and the lowest (0.0006 mg/L) was estimated at site M34 in July. Cadmium concentrations were highest at M02 throughout the year with concentrations that ranged from 0.020 to 0.39 mg/L. Concentrations decreased considerably at downstream sampling sites where estimates ranged from 0.0006 mg/L at M34 to 0.016 mg/L at M07.

The largest monthly load of cadmium in Mineral Creek was estimated at site M34 during June (1.8 lb/d), and the smallest (0.06 lb/d) was estimated

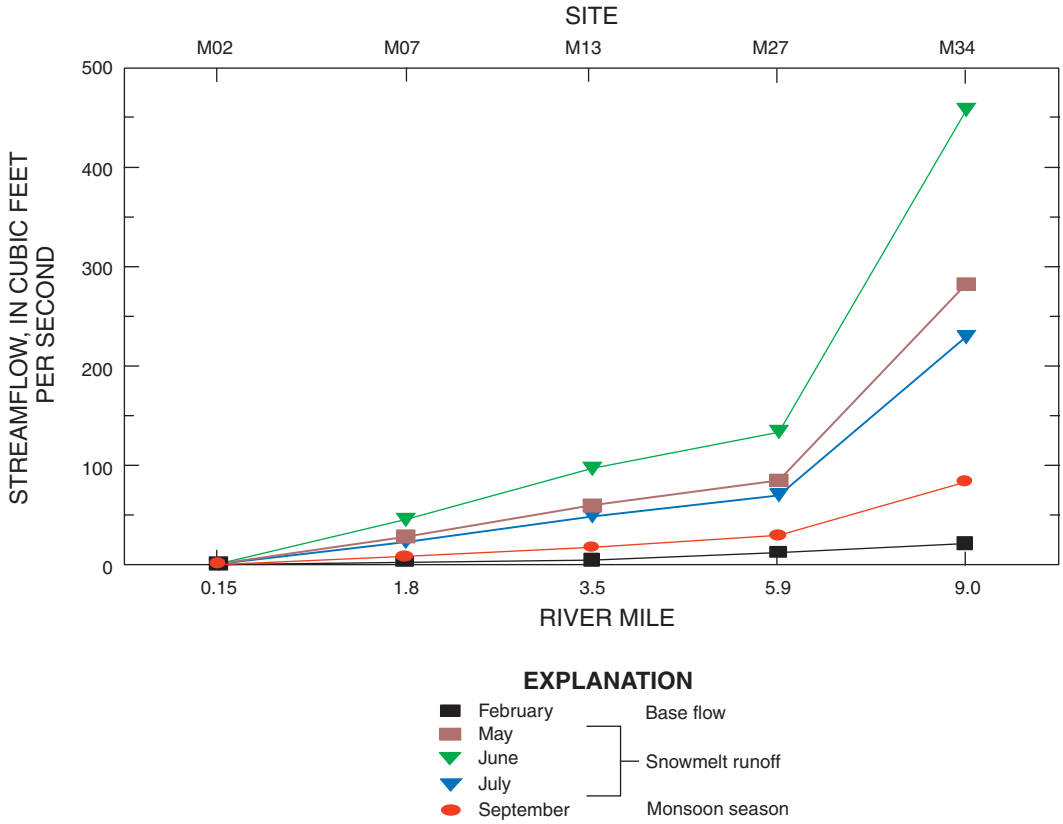

Figure 12. Streamflow profile for Mineral Creek subbasin.

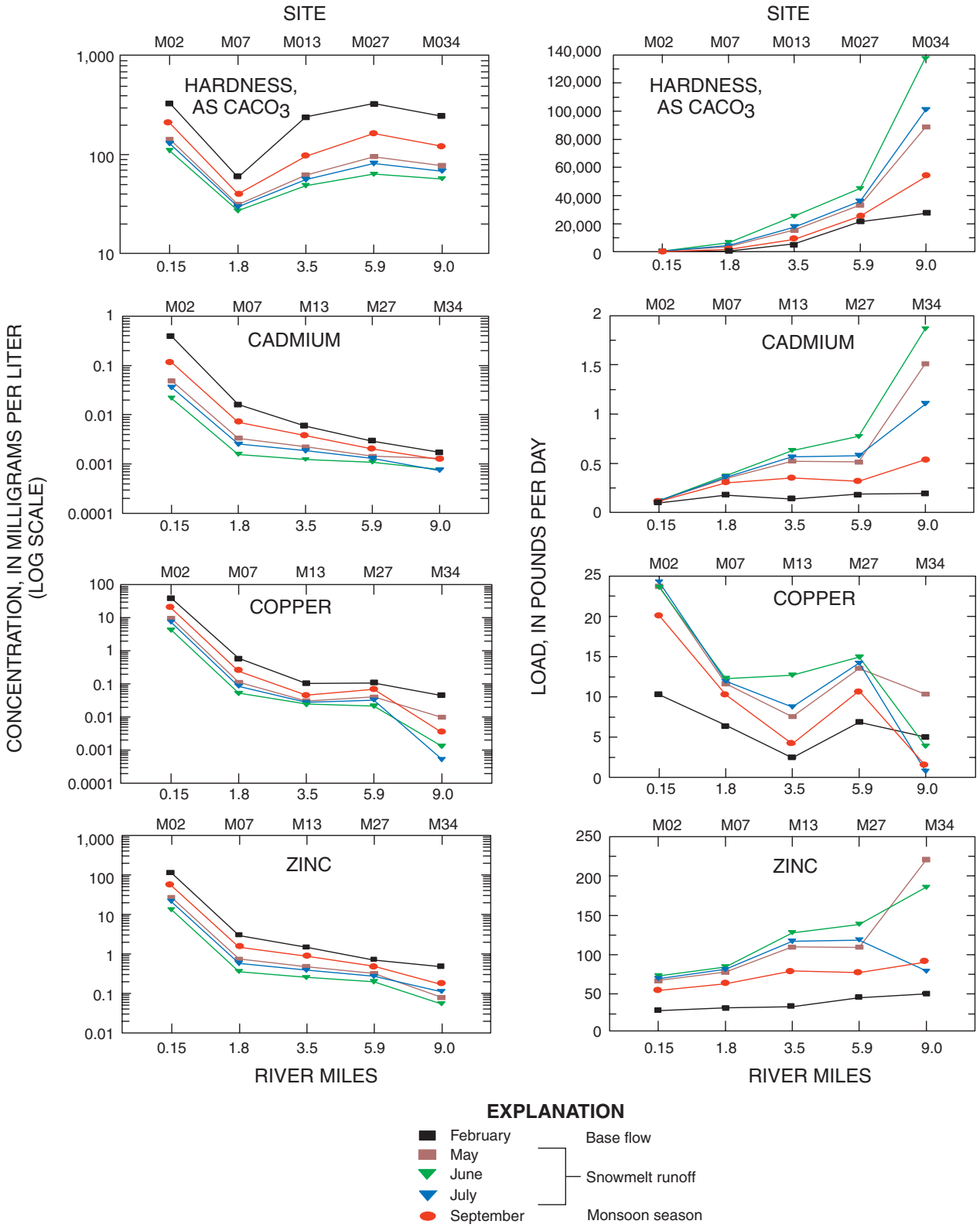

Figure 13. Water-quality profiles for hardness and dissolved cadmium, copper, and zinc at Mineral Creek sampling sites.

at site M02 in February. The largest increase in cadmium loading to Mineral Creek during base flow occurred upstream from site M02 (0.10 lb/d) and between sites M02 and M07 (0.08 lb/d). The largest increase in loading during snowmelt runoff occurred between sites M27 and M34 (0.87 lb/d). The estimates indicate that seasonal cadmium loads at the mouth of Mineral Creek subbasin (M34) account for about 15 to 25 percent of the total cadmium load at A72.

The highest monthly concentration of copper (39.8 mg/L) was estimated at site M02 in February, and the lowest (0.0004 mg/L) was estimated at site M34 in August (not shown in fig. 13). Copper concentrations were highest at M02 throughout the year with concentrations that ranged from 3.0 to 39.8 mg/L. Concentrations decreased considerably at downstream sampling sites where estimates ranged from 0.0004 mg/L at M34 to 0.6 mg/L at M07.

The largest monthly load of copper in Mineral Creek was estimated at site M02 during July (24.5 lb/d), and the smallest (2.4 lb/d) was estimated at site M13 in January. The largest increase in copper loading to Mineral Creek during base flow occurred upstream from site M02 (10 lb/d) and between sites M13 and M27 (4.5 lb/d). The largest increase of loading during snowmelt runoff primarily occurred upstream from site M02 (23 lb/d) and between sites M13 and M27 (3.3 lb/d). Stream reaches M02 through M13 and M27 to M34 showed no net loading increases during any part of the year. This does not imply that no loading is occurring in these sections but may indicate an attenuation of copper load that exceeds the rate of loading inputs from sources draining into these stream segments. Estimates indicate that seasonal copper loads at M34 account for about 31 to 65 percent of the load at A72 for any given month.

The highest monthly concentration of zinc (112 mg/L) was estimated at site M02 during February, and the lowest (0.05 mg/L) was estimated at site M34 in June. Zinc concentrations were highest at M02 throughout the year with estimates that ranged from 13.0 to 112 mg/L. Concentrations decreased considerably at downstream sampling sites where estimates ranged from 0.05 mg/L at M34 to 2.9 mg/L at M07.

The largest monthly load of zinc in Mineral Creek was estimated at site M34 during May (220 lb/d), and the smallest was estimated at site M02 in February (28 lb/d). The largest increase in zinc loading to Mineral Creek during base flow occurred between sites M13 and M27 (11.2 lb/d), and the largest increase in loading during snowmelt runoff occurred between sites M27 and M34 (39.5 lb/d). Models indicate that seasonal zinc loads at M34 account for about 10 to 27 percent of the load at A72 for any given month.

Downward trends in trace-metal concentrations were measured for zinc and copper at site M34 (fig. 14). These trends correlate to the period when the Longfellow/Koehler project was completed in fall 1997 (table 1). The project consisted of the removal of dump material near sampling site M02 that was exposed to runoff during spring snowmelt. As a result of trend detection, data collected before October 1997 were not used to derive water-quality regression models for zinc and copper at sites M02, M07, M13, and M27.

Upper Animas River

Streamflow and water-quality profiles in the upper Animas River subbasin were calculated for sites A33, A53, A60, A68, and A72 (fig. 1). Site A72, which is downstream from sites C48 and M34, was included so the combined loading from Cement and Mineral Creeks could be quantified and compared to sites upstream from A68. Inclusion of A72 also provided an indirect estimate of the effects of Cement Creek to the Animas River. Direct estimates of Cement Creek loading were not calculated because of the insignificance of the trace-element water-quality models.

Regression models at all sites in the upper Animas River subbasin (including A72) were statistically significant for streamflow, hardness, cadmium, copper, and zinc. These models had r^2 values that ranged from 0.60 to 0.98. The streamflow profile for the Animas River is shown in figure 15, and concentration and loading profiles for metals are shown in figure 16.

Two sites in the Animas River (A68 and A72) had large enough data sets to test for trends; however, no trends were detected for hardness or trace metals. This finding indicates that site A72 does not show any measurable effect from the various remediation projects performed in Mineral and Cement Creeks. This does not indicate that no effect has resulted from remediation but only that no effect has been measured. Further water-quality monitoring of this site may be necessary to detect subtle trends in concentration that may be occurring over an extended period of time.

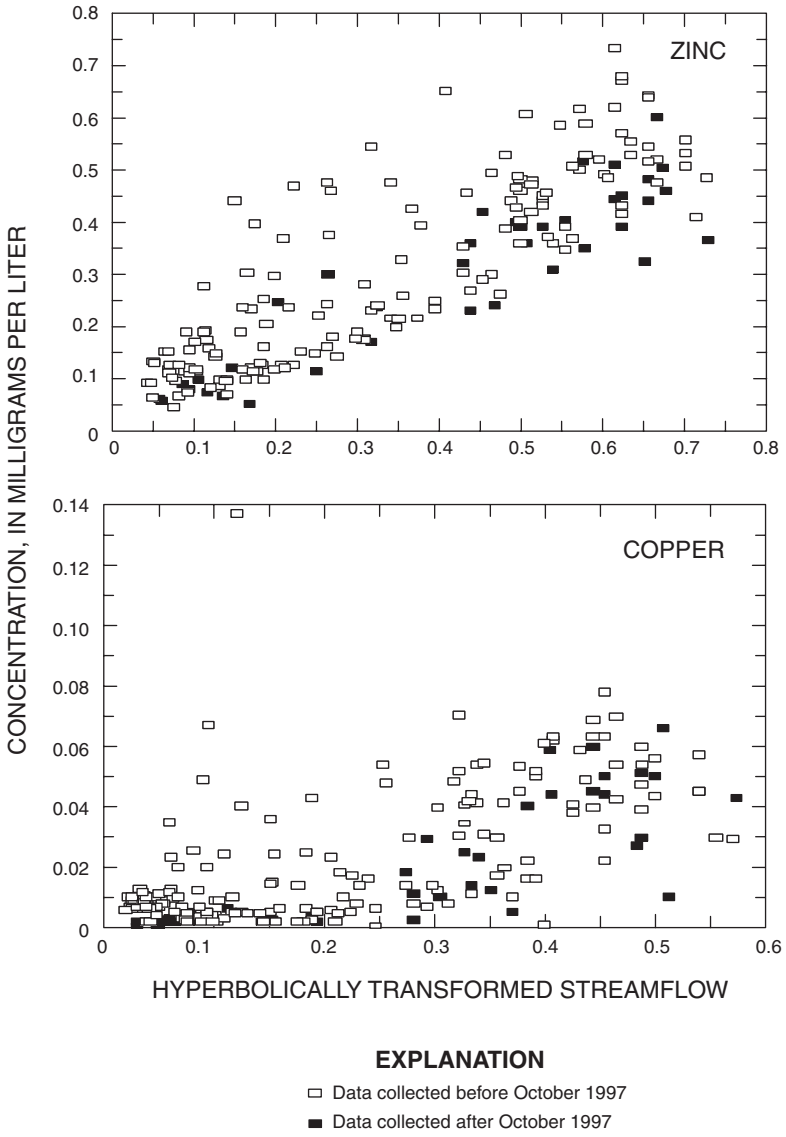

Figure 14. Trace-metal concentrations at site M34 before and after the Longfellow/Koehler project was completed in October of 1997.

The streamflow profile for the Animas River indicates that base flow ranged among sampling sites from about 0.5 ft^3/s at A33 to about 63 ft^3/s at A72. Peak snowmelt runoff generally occurred in June and ranged from about 140 ft^3/s at site A33 to 1,200 ft^3/s at A72. Simulated streamflow at the mouth of the upper Animas River subbasin (A68) accounted for about 41 to 42 percent of the total streamflow at A72, of which about 55 to 83 percent originated between sites A33 and A53. Average annual streamflow draining the upper Animas River subbasin (A68) is about 126 ft^3/s, or 1.8 cfsm.

The highest monthly concentration of hardness (291 mg/L) was estimated at site A72 in January (not shown), and the lowest (30.0 mg/L) was estimated at site A33 in June (fig. 16). Water-quality models estimated hardness concentrations that showed dilution during snowmelt runoff and concentration during base flow. At site A72 in January, estimated concentrations of hardness were approximately 150 to 180 mg/L higher than concentrations at other sampling sites in the upper Animas River subbasin despite the increase in streamflow; however, in May, concentrations at all sampling sites were within

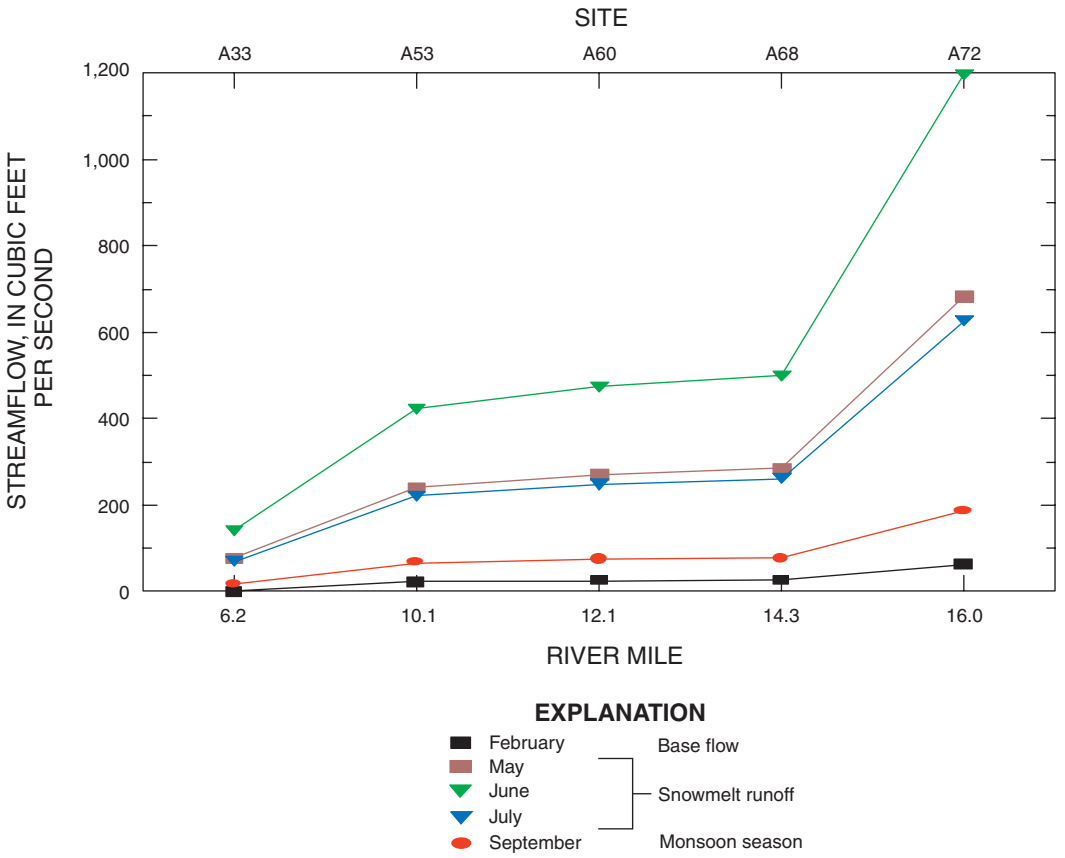

Figure 15. Streamflow profile for the Animas River.

35.0 mg/L of one another. This finding indicates the presence of hardness sources in Mineral and Cement Creeks, which could be of vital importance to aquatic habitat during base flow. The decrease in hardness detected at C20 did not noticeably alter the correlation of hardness and streamflow at A72 based on results from the trend testing performed for this study; however, additional portal closures in Mineral or Cement Creeks could theoretically increase stream toxicities in receiving waters if additional hardness sources are eliminated.

The largest monthly load of hardness in the Animas River was estimated at site A72 during June (375,000 lb/d), and the lowest (1,450 lb/d) was estimated at site A33 in February. The largest increase in loading in the Animas River during base flow and during snowmelt runoff occurred between sites A68 and A72 at 75,500 lb/d (base flow) and 187,000 lb/d (snowmelt runoff). Sources in the A68 to A72 stream segment contribute about 59 to 76 percent of the average monthly hardness load estimated at A72. Approximately two-thirds of the load in the A68 to A72 stream reach originates from Mineral Creek subbasin during snowmelt runoff, and two-thirds originates from Cement Creek during base flow.

The highest monthly concentration of cadmium (0.0028 mg/L) was estimated at site A68 during the month of March (not shown in fig. 16), and the lowest (0.0007 mg/L) was estimated at site A53 in January and February. Detection limits reported by the USGS for 1997–99 samples in the upper Animas River for cadmium were lower than those of Cement and Mineral Creek because analysis was done using GFAA (table 4). The lower detection limit improved the significance of the cadmium models because the majority of cadmium concentrations would have otherwise been below detection limits and therefore estimated. This decision was based on information gained in Mineral Creek and the awareness of low levels from preexisting data.

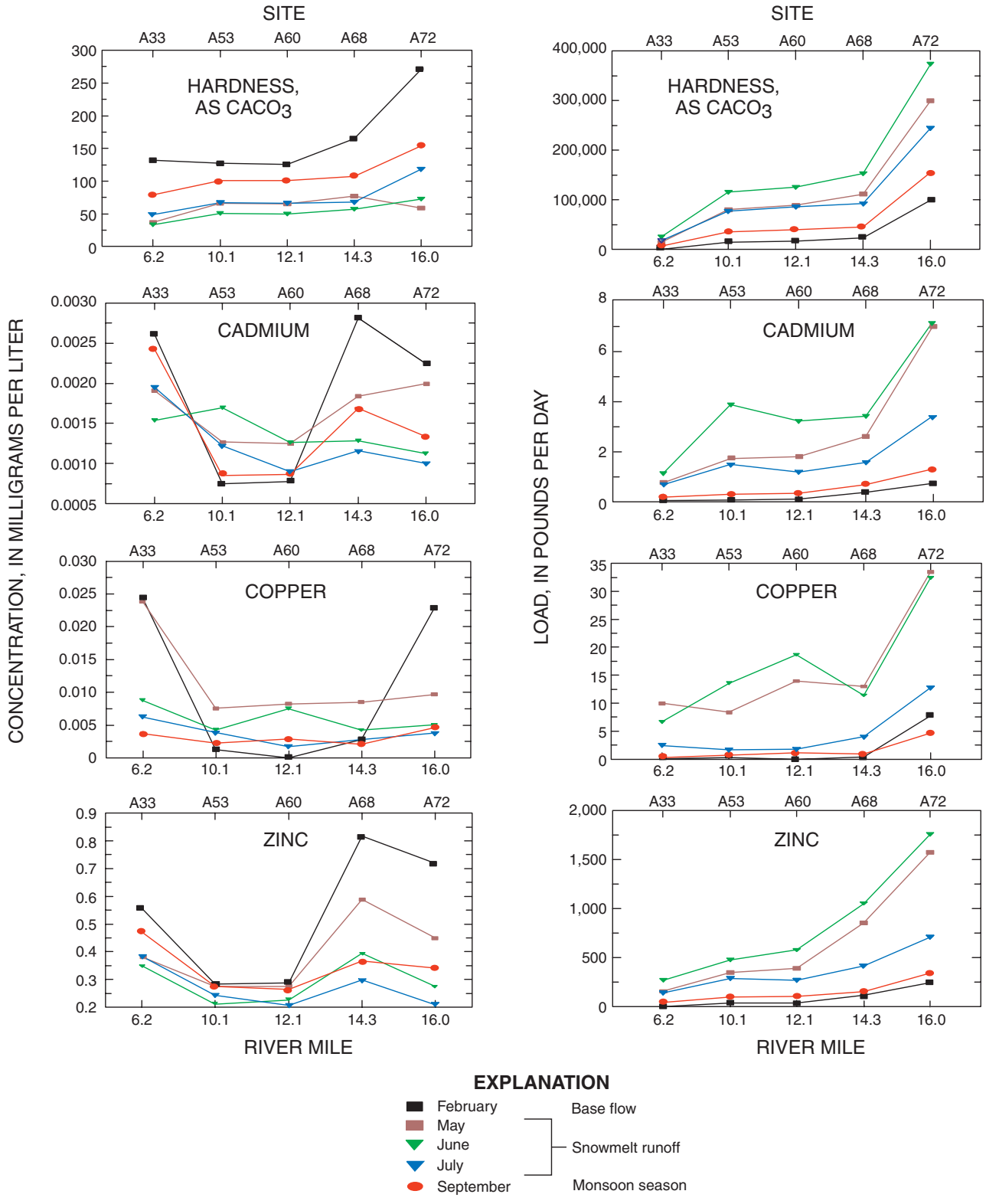

Figure 16. Water-quality profiles for hardness and dissolved cadmium, copper, and zinc at Animas River sampling sites.

A flushing variable was retained in the cadmium water-quality model after stepwise regression for May 1 through June 30 at sites A60 and A68 and for the period of April 1 to May 31 at site A72 (DV, table 8). When estimating cadmium at these sites during these months, a value of 1 is assigned to the flushing variable.

The cadmium model at site A53 estimated a positive relation of cadmium to streamflow which showed the highest cadmium concentration in June (0.0017 mg/L) and lowest in February (0.0007 mg/L). Ore mills formerly located between sites A33 and A53 supplied huge quantities of tailings to the river at rates 50 to 4,700 times greater than the natural production of sediments from hill slopes (Vincent and others, 1999). The presence of mill tailings in the flood plain may explain why there is a positive relation of cadmium concentration to streamflow because higher streamflow will tend to flush areas of the flood plain that are dry during base flow. Water-quality models for other sites estimated cadmium concentrations that showed dilution during snowmelt runoff, which was preceded by an initial flush of higher cadmium concentration.

The largest load of cadmium in the Animas River was estimated at site A72 during June (7.0 lb/d), and the lowest (0.03 lb/d) was estimated at site A33 in February. The largest increases in cadmium loading in the Animas River during base flow and during snowmelt runoff occurred between sites A68 and A72 at 0.36 lb/d (base flow) and 4.3 lb/d (snowmelt runoff). Loss of cadmium load between sites A53 and A60 may be a result of attenuation in this segment. Models indicate that cadmium loads at the mouth of the upper Animas River subbasin (A68) account for about 38 to 62 percent of the load at A72 for any given month.

The highest monthly concentration of copper (0.024 mg/L) was estimated at site A33 during February, and the lowest (0.001 mg/L) was estimated at site A60 in February. Estimated copper concentrations showed dilution during snowmelt runoff with the exception of site A72, which were preceded by an initial flush of higher copper concentration in May. The highest concentrations of copper in the upper Animas River typically occurred at the same sampling sites year-round. During base flow, the models estimated the highest concentrations of copper at site A33 (0.024 mg/L) and A72 (0.023 mg/L), during snowmelt runoff, the highest concentrations of copper (0.013 mg/L) occurred at site A33. During the monsoon season, models at site A60 estimated concentrations (0.0044 mg/L) that approached those of A33 (0.0047). The higher concentrations at A60 during the monsoon season may be occurring as a result of rainfall runoff from Arrastra Creek, which drains an area with several historical mill sites and mines where copper ore was processed.

Flushing variables were retained in several copper water-quality models after stepwise regression for the month of May at site A33, the period of May 1 to June 30 at sites A53 and A60, and April 1 to May 31 at site A68 (DV, table 8).

The largest load of copper in the Animas River was estimated at site A72 during May (33 lb/d), and the lowest (0.25 lb/d) was estimated at site A33 in February. The largest increase in copper loading in the Animas River during base flow and during snowmelt runoff occurred between sites A68 and A72 at 7.5 lb/d (base flow) and 16.7 lb/d (snowmelt runoff). Moderate gains in load (5.2 lb/d) during snowmelt runoff also occurred between A33 and A60. Estimates from models indicate that seasonal copper loads at A68 are generally about 5 to 39 percent that of the load at A72 for any given month and that the lowest percentages occur during base flow.

The highest monthly concentration of zinc (0.90 mg/L) was estimated at site A68 during April (not shown), and the lowest (0.21 mg/L) was estimated at site A60 in July. Models estimated zinc concentrations that showed dilution during snowmelt runoff and concentration during base flow.

The largest load of zinc in the upper Animas River was estimated at site A72 during June (1,750 lb/d), and the smallest (1.1 lb/d) was estimated at site A33 in February. The largest increase in zinc loading among sites during base flow and snowmelt runoff occurred between A68 and A72 at 125 lb/d (base flow) and 570 lb/d (snowmelt runoff). However, about 40 to 60 percent of the average monthly zinc load estimated at site A72 for any given month originates upstream from site A68. Thus, roughly one-half of the zinc loading at site A72 appears to be coming from Cement and Mineral Creeks and the other one-half comes from sources upstream from site A68. The largest increases in zinc loading upstream from A68 occurred between either A33 to A53 or A60 to A68 throughout the year.

APPLICATION OF WATER-QUALITY PROFILING IN MINERAL CREEK

The application presented in this section demonstrates that the results from water-quality profiling not only provide information about seasonal streamflow, concentration, and load on a watershed scale but also provide information from which to compare contaminant source loads to instream loads. This comparison is important because undetected contaminant sources (such as diffuse inputs) may be indicated when quantified contaminant sources do not account for the total instream load. This technique is generally referred to as "mass accounting;" however, this example includes a seasonal component, which quantifies the portion of source contaminants accounted for in the stream during different seasonal periods. Therefore, in addition to the information obtained from a loading profile, this application requires characterization data from contaminant sources affecting water quality.

The example stream segment was bracketed by sampling sites M27 and M34 (fig.1) in the Mineral Creek subbasin. Selection of this segment was based on the availability of source characterization data and the large downstream loading increases in May and June for cadmium and zinc (fig. 13). Changes in load were calculated from the Mineral Creek loading profiles and then compared to loading calculations from contaminant sources, which were obtained from seasonal mine-site characterization studies (Animas River Stakeholders Group, 2000; Mast and others, 2000). Monthly samples from Mast and others were used to calculate instantaneous loading values from the characterized sources in the example reach. Loading values are calculated by taking the product of concentration, flow, and a conversion constant to obtain a loading value measured in pounds per day (lb/d). These values were assumed to represent mean monthly loads from each characterized source because these were the only data available. Loading changes at main-stem sites were calculated by subtracting the constituent load at site M27 from the constituent load at M34. The resulting number is called the "net load." A positive value of net load indicates an overall gain in load for the selected stream reach. A negative value of net load indicates that the metal load is attenuated along the stream segment, typically because of adsorption and coprecipitation processes (Schemel and others, 2000). Characterized source loads were then compared to the net load. The difference between characterized source load and net load (where net load is subtracted from characterized source load) in the stream segment is referred to as the "load discrepancy." The load discrepancy indicates the portion of load at the downstream sampling site (M34) contributed by uncharacterized sources in the selected stream segment, as well as the attenuation of trace metals. Load discrepancies near 0 indicate that there are no uncharacterized sources or that a portion of the instream and(or) characterized source load is being attenuated and uncharacterized sources contribute additional loadings, which happen to equal the net load. A positive load discrepancy indicates that the net load is being attenuated and a negative load discrepancy indicates that uncharacterized sources exist.

Net loads for cadmium, copper, and zinc in the example segment between sites M27 and M34 were calculated for May and September. Loading discrepancies were evaluated by comparing all available source loading data for the reach to the net load. This stream segment had source characterization data collected at five mine portals during high streamflow and the relatively lower flows of the monsoon season (May and September). These portals represent the majority of mining effects in the stream segment; however, other diffuse sources such as in-stream waste-rock piles and ground-water inputs may exist that have not been characterized. The presence of these additional sources is assumed if the load discrepancy in this example is determined to be negative for a given metal.

From the Mineral Creek loading profile, on average during May, net loads of cadmium, copper, and zinc were 1.0 ($\pm$0.49) lb/d, –3.1 ($\pm$1.52) lb/d, and 111 ($\pm$55.4) lb/d (fig. 13), indicating a net gain for each metal, with the exception of copper, along the stream segment. Error estimates for the net loading values are reported as $\pm$ one standard deviation of the estimated net loading for the given month. Total characterized source loads in May, computed using the source characterization data for each constituent, indicated that the load discrepancy was about: (1) –0.44 to –1.42 lb/d for cadmium, (2) 5.17 to 2.14 lb/d for copper, and (3) –40.6 to –151 lb/d for zinc. The negative load discrepancies indicate that other sources contribute possibly substantial amounts of cadmium and zinc in the M27 to M34 stream segment during May, whereas the positive load discrepancy for copper indicates that attenuation is

taking place. Taking the average loading-discrepancy estimate from the above ranges for each metal indicates that the uncharacterized sources contribute nearly 95 percent of the cadmium load, 0 percent of the copper load (or uncharacterized sources also are attenuated), and about 85 percent of the zinc load at M34.

For September, net mean monthly loads of cadmium, copper, and zinc were estimated to be 0.22 (±0.12) lb/d, –9.3 (±0.27) lb/d, and 13.8 (±10.5) lb/d (fig. 13), indicating a net gain in cadmium and zinc load and a net loss of copper along the stream segment. Total characterized source loads in September indicated that the load discrepancy ranged from (1) –0.07 to –0.31 lb/d for cadmium, (2) 9.6 to 9.06 lb/d for copper, and (3) 5.01 to –16.0 lb/d for zinc. The negative load discrepancy range for cadmium indicates that other sources are contributing metals along the stream segment during September. The positive loading-discrepancy range for copper indicates an attenuation of metals from characterized sources. Zinc is more difficult to define based on the positive and negative range; however, an average value for the loading discrepancy (–5.49) indicates that additional sources may be contributing in the stream reach during September. Taking the average loading-discrepancy estimate for each constituent indicates that the uncharacterized sources contribute about 86 percent of the cadmium load, 0 percent of the copper load (or uncharacterized sources also are attenuated), and about 52 percent of the zinc load at M34.

Further characterization of the M27 to M34 segment may help explain where uncharacterized loading sources of cadmium and zinc emanate from, especially during snowmelt runoff. The results indicate these inputs may occur diffusely because the majority of surface-water sources were thought to have been accounted for. Other surface-water sources may exist, however, and there is likely some degree of flushing of attenuated metals. It also appears likely that diffuse sources of copper are not problematic in the M27 to M34 stream reach where water-column chemistry is concerned. Regardless of where these metals emanate from, mass accounting with loading profiles indicates that metal sources in the upper Animas River Basin may change substantially with season, as well as the need for further characterization studies in the example segment.

SUMMARY

Because instream water-quality standards are being proposed for the Animas River as part of the 1977 Clean Water Act (Public Law 92–500), multi-agency collaborative efforts are being made to assess the effects of historical mining on water quality in the upper Animas River Basin. Included in these efforts is the U.S. Department of the Interior Abandoned Mine Lands Initiative. As part of this initiative, the U.S. Geological Survey has provided technical assistance in support of Federal land-management agencies' actions to improve water quality in contaminated stream systems associated with abandoned hard-rock mining activities. One of the important types of information needed to characterize water quality in streams affected by historical mining is the seasonal pattern of toxic trace-metal concentrations and loads. These patterns were estimated with a technique called water-quality profiling.

Streamflow and water-quality data collected at 15 sites in the upper Animas River Basin during water years 1991–99 were used to develop water-quality profiles. Data collected at each sampling site were used to develop ordinary least-squares regression models for streamflow and water quality. Streamflow was estimated by correlating instantaneous streamflow measured at ungaged sites with continuous streamflow records from streamflow-gaging stations in the subbasin. Water-quality regression models were developed to estimate hardness and dissolved cadmium, copper, and zinc concentrations based on streamflow and seasonal terms. Results from the regression models were used to calculate water-quality profiles for streamflow and select constituent concentrations and loads.

Trends in streamflow and water quality were detected at three locations in the Animas Basin. A downward trend in streamflow was detected at site C20, which may have resulted when the American Tunnel bulkhead was closed in September 1996. Data at sites C20 and C48 indicated a decrease in hardness concentrations, which also correlates to the period when the American Tunnel was closed. Data collected at site M34 indicated a decrease in copper and zinc concentrations, which correlated to the period when the Longfellow/Koehler project was completed in fall 1997.

Hardness estimates at all sampling sites in the Animas Basin indicated that concentrations were generally highest in Cement Creek and lowest in the upper Animas River. At sampling sites in each subbasin, models estimated hardness concentrations that varied substantially during base flow and moderately during snowmelt runoff.

Inputs of hardness loading to Cement Creek were highest between sites C18 and C20 during snowmelt runoff; however, loading inputs were fairly proportional the rest of the year among sites. The largest increases of hardness load in Mineral Creek were estimated to be occurring between sites M27 and M34 during snowmelt runoff and between sites M13 and M27 during base flow. The largest increases of hardness loads in the upper Animas River occurred between sites A68 and A72 during base flow and snowmelt runoff. The largest increases of hardness load estimated upstream from A68 occurred between A33 and A53 throughout the year.

A summary of results from the water-quality profiles indicates that cadmium concentrations and loads estimated in Mineral Creek and the upper Animas River were generally higher at Mineral Creek sites; however, concentrations at site A68 exceeded those estimated at site M34 throughout the year. Model estimates at site A53 showed a positive relation of cadmium concentration to streamflow. Flushing of cadmium at sampling sites in the Animas River was readily apparent from the models and raw data, whereas flushing of cadmium in Mineral Creek was less extensive.

The largest increase of cadmium load in Mineral Creek was estimated between sites M27 and M34 during snowmelt runoff. Cadmium loads in the upper Animas River were largest between sites A68 and A72 throughout the year.

Copper concentrations estimated for Mineral Creek and the upper Animas River indicated that concentrations were significantly higher at Mineral Creek sites. Estimates of copper concentration at upper Animas River sampling sites were generally highest in May as a result of flushing, but concentrations in Mineral Creek were highest during the later part of the base-flow period.

The largest increases of copper load in Mineral Creek were estimated to be occurring upstream from site M02 and between sites M13 and M27 throughout the year. The largest increases of copper load in the upper Animas River occurred between sites A68 and A72 and to a lesser extent between A33 and A60 during snowmelt runoff.

In Cement Creek subbasin (C18 and C20), the highest zinc concentrations were estimated at site C18 throughout the year. Concentrations at site C18 were highest during base flow, whereas concentrations at site C20 were lowest during this period. This may be a result of the water-treatment plant located between sites C18 and C20. The plant treats most of the water in Cement Creek during base flow (winter), but does not have the capacity to treat all the streamflow during snowmelt runoff. Zinc concentrations estimated for Mineral Creek and the upper Animas River indicated that concentrations in Mineral Creek decrease in a downstream fashion, whereas in the upper Animas River, concentrations increased substantially between sites A60 and A68 despite increases estimated by the streamflow profile. Zinc concentrations in Mineral Creek were not elevated during spring snowmelt by flushing events, but zinc concentrations in the Animas River showed this effect.

The largest zinc load in Cement Creek was estimated to be occurring upstream from site C18 throughout the year. Between C18 and C20, decreases in zinc load were estimated during base flow. The largest increases of zinc load in Mineral Creek were between sites M27 and M34 and upstream from site M02 during snowmelt runoff. The largest increases of zinc load during base flow and snowmelt runoff in the upper Animas River occurred between sites A68 and A72; however, loading of zinc upstream from A68 accounts for approximately 40 to 60 percent of zinc load at A72.

Quantification of cadmium, copper, and zinc loads in a stream segment in Mineral Creek (M27 to M34) was presented as an example application of water-quality profiling. The application used a method of mass accounting to quantify the portion of metal loading in the segment derived from uncharacterized sources during different seasonal periods. During May, uncharacterized sources contributed nearly 95 percent of the cadmium load, 0 percent of the copper load (or uncharacterized sources also are attenuated), and about 85 percent of the zinc load at M34. During September, uncharacterized sources contributed about 86 percent of the cadmium load, 0 percent of the copper load (or uncharacterized sources also are attenuated), and about 52 percent of the zinc load at M34. Characterized sources accounted for more of the loading gains estimated in the example reach during September, possibly indicating the presence of diffuse inputs during snowmelt runoff. Regardless of where the sources emanate from, the results indicate that metal sources in the upper Animas River Basin may change substantially with season.

REFERENCES CITED

Animas River Stakeholders Group, 2000, Animas River Basin database at URL: http://www.waterinfo.org/arsg/main.html, accessed 1997–2000.

Anderson, S.P., Dietrich, W.E., Torres, R., Montgomery, D.R., and Loague, K., 1997, Concentration discharge relationships in runoff from a steep, unchanneled catchment: Water Resources Research, v. 33, p. 211–225.

Aulenbach, B.T., and Hooper, R.P., 1994, Adjusting solute fluxes for climatic influences: American Geophysical Union 1994 fall meeting, Eos Transactions, Washington, D.C., p. 233.

Bailey, R.G., Avers, P.E., King, T., and McNab, W.H., eds., 1994, Ecoregions and subregions of the United States with supplementary table of map unit descriptions: Washington, D.C., U.S. Department of Agriculture Forest Service, scale 1:7,500,000 (also at URL <http://www.fs.fed.us/land/ecosysmgmt/ecoreg1_home.html>) accessed 1999.

Besser, J.M., and Leib, K.J., 1999, Modeling frequency of occurrence of toxic concentrations of zinc and copper in the Upper Animas River, *in* Morganwalp, D.W., and Buxton, H.T., eds., U.S. Geological Survey Toxic Substances Hydrology program—Proceedings of the Technical Meeting, Charleston, S.C., March 8–12, 1999: U.S. Geological Survey Water-Resources Investigations Report 99–4018A, p. 75–81.

Casadevall, T.J., and Ohmoto, H., 1977, Sunnyside Mine, Eureka Mining District, San Juan County, Colorado—Geochemistry of gold and base metal ore deposition in a volcanic environment: Economic Geology, v. 72, p. 1285–1320.

Colorado Climate Center, 2000, Annual climatology data at URL: http://climate.atmos.colostate.edu/ accessed May 2000.

Colorado Department of Public Health and Environment, 1995, Classification and numeric standards for San Juan and Dolores River basins: Water Quality Control Commission, regulation notice 3.4.0, 65 p.

Crawford, C.G., Slack, J.R., and Hirsch, R.M., 1983, Nonparametric tests for trends in water-quality data using the Statistical Analysis System: U.S. Geological Survey Water-Supply Paper 83–550, 48 p.

Driver, N.E., and Tasker, G.D., 1990, Techniques for estimation of storm-runoff loads, volumes, and selected constituent concentrations in urban watersheds in the United States: U.S. Geological Survey Water-Supply Paper 2363, 44 p.

Duan, Naihua, 1983, Smearing estimate—A nonparametric retransformation method: Journal of the American Statistical Association, v. 78, no. 383, p. 605–610.

Dunne, Thomas, and Leopold, L.B., 1978, Water in environmental planning: New York, W.H. Freeman and Company, 818 p.

Edwards, T.K., and Glysson, G.D., 1988, Field methods for measurement of fluvial sediment: U.S. Geological Survey Open-File Report 86–531, 118 p.

Helsel, D.R., and Hirsch, R.M., 1992, Statistical methods in water resources: New York, Elsevier, 522 p.

Hem, J.D., 1985, Study and interpretation of the chemical characteristics of natural water: U.S. Geological Survey Water-Supply Paper 2254, 263 p.

Johnson, N.M., Likens, G.F., Borman, F.H., Fisher, D.W., and Pierce, R.S., 1969, A working model for the variation in stream water chemistry at the Hubbard Brook Experimental Forest, New Hampshire: Water Resources Research, v. 5, p. 1353–1363.

Luedke, R.G., and Burbank, W.S., 1996, Preliminary geologic map of the Silverton 7.5-minute quadrangle, San Juan County, Colorado: U.S. Geological Survey Open-File Report 96–275, 15 p., 1 pl.

Mast, M.A., Evans, J.B., Leib, K.J., and Wright, W.G., 2000, Hydrologic and water-quality data at selected sites in the upper Animas River watershed, southwestern Colorado, 1997–99: U.S. Geological Survey Open-File Report 00–53, 24 p., 1 pl., appendix on compact disc.

Nimick, D.A., and von Guerard, P.B., 1998, Science for watershed decisions on abandoned mine lands—Review of preliminary results: U.S. Geological Survey Open-File Report 98–297, 47 p.

Ott, L.R., 1993, An introduction to statistical methods and data analysis (4th ed.): Belmont, Calif., Wadsworth Publishing, 1050 p.

Schemel, L.E., Kimball, B.A., and Bencala, K.E., 2000, Colloid formation and metal transport through two mixing zones affected by acid mine drainage near Silverton, Colorado: Applied Geochemistry, v. 15, p. 1003–1018.

Searcy, J.K., 1959, Flow-duration curves: U.S. Geological Survey Water-Supply Paper 1542–A, 33 p.

SPSS Inc., 1997a, SYSTAT 7.0 software: SPSS Inc., Chicago, Ill.

———1997b, SYSTAT 7.0, users guide—Statistics: SPSS Inc., United States of America, 751 p.

Steele, T.D., 2000, Estimation of solute loading: American Water Resources Association, 2000 Annual Symposium, March 17, 2000, Golden, Colo., 48 p.

U.S. Geological Survey, 1991–2000, Water resources data for Colorado, water years, 1992–99—v. 2, Colorado River Basin: U.S. Geological Survey Water-Data Reports CO–92–2 to CO–99–2 (published annually).

Vincent, K.R., Church, S.E., and Fey, D.L., 1999, Geomorphological context of metal-laden sediments in the Animas River flood plain, Colorado, *in* Morganwalp, D.W., and Buxton, H.T., eds., U.S. Geological Survey Toxic Substances Hydrology Program—Proceedings to the Technical Meeting, Charleston, S.C., March 8–12, 1999: U.S. Geological Survey Water-Resources Investigations Report 99–4018A, p. 99–105.

Varnes, D.J., 1963, Geology and ore deposits of the South Silverton mining area, San Juan County, Colorado: U.S. Geological Survey Professional Paper 378–A, 53 p., 7 pl.

Wetherbee, G.A., and Kimball, B.A., 1989, Use of environmental variables to estimate metal loads in streams, upper Arkansas River Basin, Colorado, *in* Mallard, G.E., and Aronson, D.A., eds., U.S. Geological Survey Toxic Substances Hydrology Program—Proceedings to the Technical Meeting, Monterey, Calif., March 11–15, 1991: U.S. Geological Survey Water-Resources Investigations Report 91–4034, p. 398–406.

Wilde, F.D., and Radtke, D.F., 1997, National field manual for the collection of water-quality data: U.S. Geological Survey Techniques of Water-Resources Investigations, book 9, chap. A6, variously paged.

Wirt, Laurie, Leib, K.J., Bove, D.J., Mast, M.A., Evans, J.B., and Meeker, G.P., 1999, Determination of chemical-constituent loads during base-flow and storm-runoff conditions near historical mines in Prospect Gulch, upper Animas River watershed, southwestern Colorado: U.S. Geological Survey Open-File Report 99–0159, 39 p.

APPENDIX

Appendix. State of Colorado table value standards for trace metals affected by hardness concentration

[Modified from Colorado Department of Public Health and Environment, 1995, classification and numeric standards for San Juan and Dolores River Basins: Water Quality Control Commission, regulation notice 3.4.0, 65 p.; μg/L, microgram per liter; dis, dissolved]

Metal[1]	Aquatic life[1,3,4,D]		Agriculture[2]	Drinking-water supply[2]
	Acute (μg/L)	Chronic (μg/L)		
Cadmium	(1.13667–[(ln hardness)× (0.04184)]) × $\mathbf{e}^{(1.128[\ln(\text{hardness})]-3.6867)}$ (Trout)=(1.13667–[(ln hardness)×(0.04184)])× $\mathbf{e}^{(1.128[\ln(\text{hardness})]-3.828)}$	(1.10167–[(hardness)× (0.04184)])× $\mathbf{e}^{(0.7852[\ln(\text{hardness})]-2.715)}$	10^{A} (30-day)	5.0^{B} (1-day)
Chromium III[5]	$\mathbf{e}^{(0.819[\ln(\text{hardness})]+2.5736)}$	$\mathbf{e}^{(0.819[\ln(\text{hardness})]+0.5340)}$	100^{A} (30-day)	50^{B} (1-day)
Copper	$\mathbf{e}^{(0.9422[\ln(\text{hardness}-1.7408)}$	$\mathbf{e}^{(0.8545[\ln(\text{hardness})]-1.7428)}$	200^{A}	$1{,}000^{B}$ (30-day)
Lead	(1.46203–[(ln hardness)× (0.145712)])× $\mathbf{e}^{(1.273[\ln(\text{hardness})]-1.46)}$	(1.46203–[(ln hardness)× (0.145712)])× $\mathbf{e}^{(1.273[\ln(\text{hardness}-4.705)}$	100^{A} (30-day)	50^{B} (1-day)
Manganese	$\mathbf{e}^{(0.3331[\ln(\text{hardness})]+6.4676)}$	$\mathbf{e}^{(0.3331[\ln(\text{hardness})]+5.8743)}$	200^{A} (30-day)	$50(\text{dis})^{C}$ (30-day)
Nickel	$\mathbf{e}^{(0.846[\ln(\text{hardness})]+2.253)}$	$\mathbf{e}^{(0.846[\ln(\text{hardness})]+0.0554)}$	200^{A} (30-day)	100^{B} (30-day)
Silver	$\frac{1}{2}\mathbf{e}^{(1.72[\ln(\text{hardness})]-6.52)}$	$\mathbf{e}^{(1.72[\ln(\text{hardness})]-9.06)}$ (Trout) = $\mathbf{e}^{(1.72[\ln(\text{hardness})]-10.51)}$		100^{C} (1-day)
Uranium	$\mathbf{e}^{(1.1021[\ln(\text{hardness})]+2.7088)}$	$\mathbf{e}^{(1.102[\ln(\text{hardness})]+2.2382)}$		
Zinc	$\mathbf{e}^{(0.8473[\ln(\text{hardness})]+0.8618)}$	$\mathbf{e}^{(0.8473[\ln(\text{hardness})]+0.8699)}$	$2{,}000^{A}$ (30-day)	$5{,}000^{C}$ (30-day)

[1]Metals for aquatic-life use are stated as dissolved unless otherwise specified.

[2]Metals for agricultural and domestic uses are stated as total recoverable unless otherwise specified.

[3]Hardness values to be used in equations are in milligrams per liter as calcium carbonate and shall be no greater than 400 mg/L. The hardness values used in calculating the appropriate metal standard should be based on the lower 95-percent confidence limit of the mean hardness value at the periodic low-flow criterion as determined from a regression analysis of site-specific data. Where insufficient site-specific data exist to define the mean hardness value at the periodic low-flow criterion, representative regional data shall be used to perform the regression analysis. Where a regression analysis is not appropriate, a site-specific method should be used. In calculating a hardness value, regression analysis should not be extrapolated past the point that data exist.

[4]Both acute and chronic numbers adopted as stream standards are levels not to be exceeded more than once every 3 years on the average.

[5]Unless the stability of the chromium valence state in receiving waters can be clearly demonstrated, the standard for chromium should be in terms of chromium VI. In no case can the sum of the in-stream levels of hexavalent and trivalent chromium exceed the water-supply standard of 50 μg/L total chromium in those waters classified for domestic water use.

[A]EPA—Water Quality Criteria 1972, Ecological Research Series, National Academy of Sciences, National Academy of Engineering, EPA–R3–73–033, March 1973, Washington, D.C., 594 p.

[B]EPA National Interim Primary Drinking Water Regulations, 40 Code of Federal Regulations, Part 141.

[C]EPA, March 1977, Proposed National Secondary Drinking Water Regulation, Federal Register, v. 42, no. 62, p. 17143–17147.

[D]Final Report of the Water Quality Standards and Methodologies Committee to the Colorado Water Quality Control Commission, June 1986.